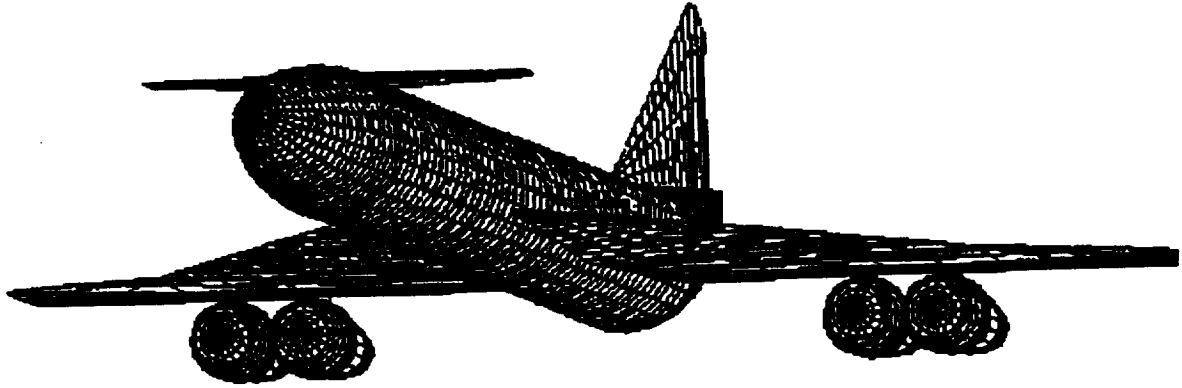


NASW-4435

1N-05-CR  
141660

P-120

# Phoenix



## *Preliminary Design of a High Speed Civil Transport*

**Presented to:**

**Professor Robert van't Riet**

**Dr. Doral Sandlin**

**Aeronautical Engineering Department  
California Polytechnic State University**

**San Luis Obispo, California**

**June 9, 1992**

**Phoenix Design Team:**

**Joseph Aguilar**

**Steven Davis**

**Brian Jett**

**Leslie Ringo**

**John Stob**

**Bill Wood**

N93-17976

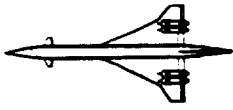
Unclas

G3/05 0141660

(NASA-CR-192024) PHOENIX:  
PRELIMINARY DESIGN OF A HIGH SPEED  
CIVIL TRANSPORT (California  
Polytechnic State Univ.)

1181

4272



# *Phoenix*

## Abstract

The goal of the Phoenix design project was to develop a second generation high speed civil transport (HSCT) that will meet the needs of the traveler and airline industry beginning in the 21st century. The primary emphasis of this HSCT is to take advantage of the growing needs of the Pacific Basin and the passengers who are involved in that growth. A passenger load of 150 persons, a mission range of 5150 nautical miles, and a cruise speed of Mach 2.5 constitutes the primary design points of this HSCT. The design concept is made possible with the use of a well designed double delta wing and four mixed flow engines. Passenger comfort, compatibility with existing airport infrastructure, and costs competitive with current subsonic aircraft make the Phoenix a viable aircraft for the future.

## Table of Contents

	Table of Contents	i
	List of Figures	iv
	List of Tables	vii
	Nomenclature	ix
1.0	Introduction	1
2.0	Mission Description	5
3.0	Preliminary Sizing	8
4.0	Configuration	12
4.1	Fuselage Configuration	12
4.2	Flight Deck	15
4.3	Interior Layout	15
4.4	Wing Design	20
4.5	Empennage Design	25
4.6	Engine Placement	27
5.0	Aerodynamics	29
5.1	Fuselage Aerodynamics	29
5.2	Wing Parameters	30
5.3	High Lift Devices	33
5.4	Control Surface Sizing	36
6.0	Drag Determination	39
6.1	Zero Lift Drag	39
6.2	Drag Due to Lift	40
6.3	Lift to Drag Ratios	41
7.0	Propulsion Integration	44
7.1	Selection of Engines	44
7.2	Inlet Placement	49
7.3	Inlet Design	50
7.4	Noise Requirements	50
8.0	Structures	51
8.1	Material Selection	51
8.2	Wing Structure	53

8.3	Fuselage	54
8.4	Canards	55
8.5	Vertical Tail	57
8.6	V-n Diagram	57
9.0	Systems Integrations	59
9.1	Air Conditioning System	59
9.2	Anti-Icing System	59
9.3	Electrical System	60
9.4	Hydraulic System	60
9.5	Fuel System	60
9.6	Water System	61
9.7	Avionics Systems	62
9.7.1	Communications	62
9.7.2	Navigation	62
9.7.3	Data Processing and Display	63
9.8	Flight Control System	63
10.0	Landing Gear	65
10.1	Configuration	65
10.2	Compliance	68
11.0	Stability and Control	71
11.1	Weight and Balance	71
11.2	Moments of Inertia	73
11.3	Excursion Plot	73
11.4	Static Stability	74
11.5	Dynamic Stability	77
11.6	Canard and Empennage Design	80
12.0	Performance	82
12.1	Takeoff and Landing	82
12.2	Climb	85
12.3	Fuel Consumption	85
12.4	Level Acceleration	85
12.5	Performance Summary	86
13.0	Airport Compatibility	87
13.1	Noise	87
13.2	Space Compliance	87
13.3	Maneuverability	87

14.0	Service Requirements and Maintenance	88
14.1	Service Requirements	88
14.2	Maintenance	88
15.0	Cost Analysis	91
15.1	Life Cycle Cost	91
15.2	Operation and Support	94
16.0	Manufacturing and Production Breakdown	97
16.1	Manufacturing	97
16.2	Production Schedule	98
17.0	Conclusions	100
18.0	References	102

## List of Figures

1.0	Introduction		
	Figure 1.0.1	Phoenix Three-View	4
2.0	Mission Description		
	Figure 2.0.1	Phoenix Mission Profile	6
3.0	Preliminary Sizing		
	Figure 3.0.1	Sizing Matrix Plot	9
4.0	Configuration		
	Figure 4.1.1	Structural Cutaway	12
	Figure 4.2.1	Flight Deck Configuration	15
	Figure 4.3.1	First Class Cross Section	16
	Figure 4.3.2	Business Class Cross Section	17
	Figure 4.3.3	Inboard Layout	19
	Figure 4.4.1	Chordwise Flow Velocity	21
	Figure 4.4.2	Planform Geometry Candidates	22
5.0	Aerodynamics		
	Figure 5.1.1	Phoenix Area Distribution	30
	Figure 5.2.1	Wing Geometry	32
	Figure 5.3.1	Typical Vortices Formation	34
	Figure 5.3.2	Leading Edge High Lift Devices	35
	Figure 5.4.1	Control Surface Arrangement	37
6.0	Drag Determination		
	Figure 6.3.1	Initial Climb Drag Polar	41
	Figure 6.3.2	Subsonic Cruise Drag Polar	42
	Figure 6.3.3	Cruise Drag Polar	43
7.0	Propulsion Integration		

	Figure 7.1.1	Mixed Flow Turbofan Geometry	45
8.0	Structures		
	Figure 8.1.1	Aircraft Temperatures	51
	Figure 8.1.2	Exterior Materials	52
	Figure 8.1.3	Interior Materials	53
	Figure 8.2.1	Wing Structural Layout	53
	Figure 8.3.1	Frame/Stringer Geometry	55
	Figure 8.3.2	Frames and Stringers	56
	Figure 8.4.1	Canard Structure	57
	Figure 8.6.1	V-n Diagram for gust at Sea-level to 20,000 Feet	58
	Figure 8.6.2	V-n Diagram for gust at 60,000 Feet	58
10.0	Landing Gear		
	Figure 10.1.1	Landing Gear Layout	65
	Figure 10.1.2	Main Landing Gear Retraction Scheme	67
	Figure 10.1.3	Main Landing Gear Retraction Path	68
	Figure 10.2.1	Tip-Over and Takeoff Rotation	69
	Figure 10.2.2	Turn-Over Criterion	70
11.0	Stability and Control		
	Figure 11.3.1	Excursion Plot	74
12.0	Performance		
	Figure 12.1.1	Takeoff Performance	82
	Figure 12.1.2	Lift and L/D During Roll	83
	Figure 12.1.3	OEI Performance for Landing	84
14.0	Service Requirements and Maintenance		
	Figure 14.1.1	Aircraft Servicing Diagram	88
	Figure 14.2.1	Wing Access Panels	89
	Figure 14.2.2	Engine Access Panels	90
	Figure 14.2.3	Major Fuselage Access Panels	90

## 15.0 Cost Analysis

Figure 15.1.1	Life Cycle Cost Breakdown	93
Figure 15.1.2	Life Cycle Cost Percentage Breakdown	94
Figure 15.2.1	Direct Operating Cost Breakdown	96

## 16.0 Manufacturing

Figure 16.1.1	Manufacturing Breakdown	97
---------------	-------------------------	----



## List of Tables

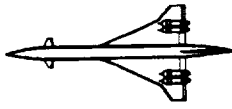
3.0	Preliminary Sizing	
	Table 3.0.1	Mission Parameters 8
	Table 3.0.2	Gross Takeoff Weight Sensitivities 11
	Table 3.0.3	Final Sizing Results 11
4.0	Configuration	
	Table 4.1.1	Fuselage Trade Study 14
	Table 4.3.1	Seat Dimensions 18
	Table 4.4.1	Wing Trade Study 24
	Table 4.5.1	Empennage Trade Study 26
5.0	Aerodynamics	
	Table 5.2.1	Wing Parameters 33
	Table 5.3.1	High Lift Device Parameters 36
6.0	Drag Determination	
	Table 6.1.1	Component Wetted Areas 39
	Table 6.3.1	Drag Characteristics 41
7.0	Propulsion Integration	
	Table 7.1.1	NASA MFT Characteristics 44
	Table 7.1.2	Engine Trade Study 46
10.0	Landing Gear	
	Table 10.1.1	Landing Gear Tire Data 66
11.0	Stability and Control	
	Table 11.1.1	Aircraft Weight Breakdown 71
	Table 11.1.2	Aircraft Weight Component Breakdown and Location 72
	Table 11.2.1	Moments of Inertia 73

Table 11.4.1	Longitudinal - Directional Stability Derivatives	75
Table 11.4.2	Lateral Directional Stability Derivatives	76
Table 11.5.1	Literal Factors for Varying Flight Conditions	77
Table 11.5.2	Dynamic Lateral-Directional Stability Results	80
12.0	Performance	
Table 12.5.1	Performance Summary	86
15.0	Cost Analysis	
Table 15.1.1	Life Cycle Cost Breakdown	92
Table 15.2.1	Direct Operating Costs	95
16.0	Manufacturing and Production Breakdown	
Table 16.2.1	Production Schedule	99

## Nomenclature

ac	aerodynamic center
AGL	Above Ground Level
APU	Auxiliary Power Unit
AR	Aspect Ratio
c	root chord
Cd	Coefficient of drag
Cdi	coefficient of induced drag
cg	center of gravity
Cl	Coefficient of lift
d	diameter
EHS	Electro-hydrostatic actuators
ESWL	Equivalent Single Wheel Landing
FCS	flight control system
FLG	Front Landing Gear
ft	feet
GE	General Electric
GPS	Global Positioning System
hr.	hour
HSCT	High Speed Civil Transport
in.	inches
KLAS	Knots Indicated Air Speed
L/D	Lift to Drag ratio
lbs.	pounds
LCN	Load Classification Number
M	Mach Number
MFE	Mixed Flow Engine
MLG	Main Landing Gear
MSL	Mean Sea Level
nmi	nautical miles
OEI	One Engine Inoperative
P&W	Pratt and Whitney
pax	passengers
psf	pounds per square foot
Ref	Reference
RR	Rolls Royce

Sref	wing reference area
SST	Supersonic Transport
STFF	Supersonic Through Flow Fan
t/c	thickness ratio
t/o	takeoff
TACAN	Tactical Aircraft Navigation aid
TBE	Turbine Bypass Engine
TF	Tandem Fan Engine
TSFC	Thrust Specific Fuel Consumption
UHF	Ultra High Frequency radio
V	Velocity
V1	decision speed
V2	rotation speed
V3	liftoff speed
VHF	Very High Frequency radio
w/s	wing loading



## 1.0 Introduction

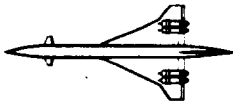
Expected increases in passenger traffic for transoceanic flights by the year 2000 demands a closer look at a second generation high-speed civil transport (HSCT). The majority of the increases in passenger traffic will occur in the trans-Pacific and trans-Atlantic routes. An economically viable HSCT would quickly capture the majority of this market.

The main advantage of an HSCT is the dramatic reduction in flight times. Using an HSCT, one day intercontinental round-trips become a reality. For this reason, the target market for this aircraft will be primarily the first class and business flier. Additional markets would be the occasional tourist flier or group trips.

To be economically viable, a second generation HSCT would have to be fully compatible with today's major airports. It should not require special or extraordinary facilities for maintenance and fueling. It would be necessary to absorb a fare surcharge to be profitable. These are the parameters in which the preliminary design of the Phoenix is made.

Aircraft design, especially in a classroom setting, relies heavily on existing aircraft as examples. For commercial HSCTs there is only one aircraft that has actually seen service, the Concorde. The Concorde has been in limited service for British Airways and Air France for almost two decades. The Concorde is seen as both a triumph and a failure.

From a technological standpoint, the Concorde was a triumph. It transports over 100 people across the Atlantic in just a couple of hours. For the airlines, the Concorde was a financial success. Due to its



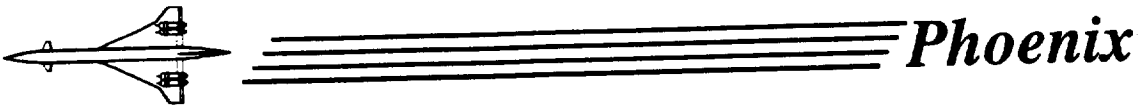
# Phoenix

uniqueness and the few Concorde actually in service, the airlines can successfully charge much higher rates than other subsonic aircraft.

From a manufacturing standpoint, the Concorde was a disaster. Only 15 production model Concorde were ever made. It's obvious that many more aircraft were necessary before the manufacturer would break even. Also, because the aircraft was so loud, the only airport in the United States that would allow it to land was New York's Kennedy Airport. This isolated the Concorde from most of the U.S. market. Most countries also banned supersonic flight overland. This altered the flight paths that an airliner would normally take, further reducing its marketability. Clearly a second generation HSCT would have to address these problems.

The Phoenix is an aircraft that can succeed where the Concorde failed. It is a true second generation HSCT. The Phoenix can transport 152 people up to 5,150 miles at speeds of up to Mach 2.5 in luxurious comfort. Supersonic flight over land is still prohibited by the majority of countries around the world. The Phoenix will overcome this loss of flight paths by concentrating on the transoceanic routes. This will take full advantage of its supersonic speed. The Phoenix also has acceptable subsonic performance. This will enable it to successfully compete with subsonic aircraft on routes that are partially over land. Using its mixed flow turbofan engines, the Phoenix will meet the stringent FAR 36 Stage III noise requirements. This will allow it to land at airports the world over, further increasing its market share.

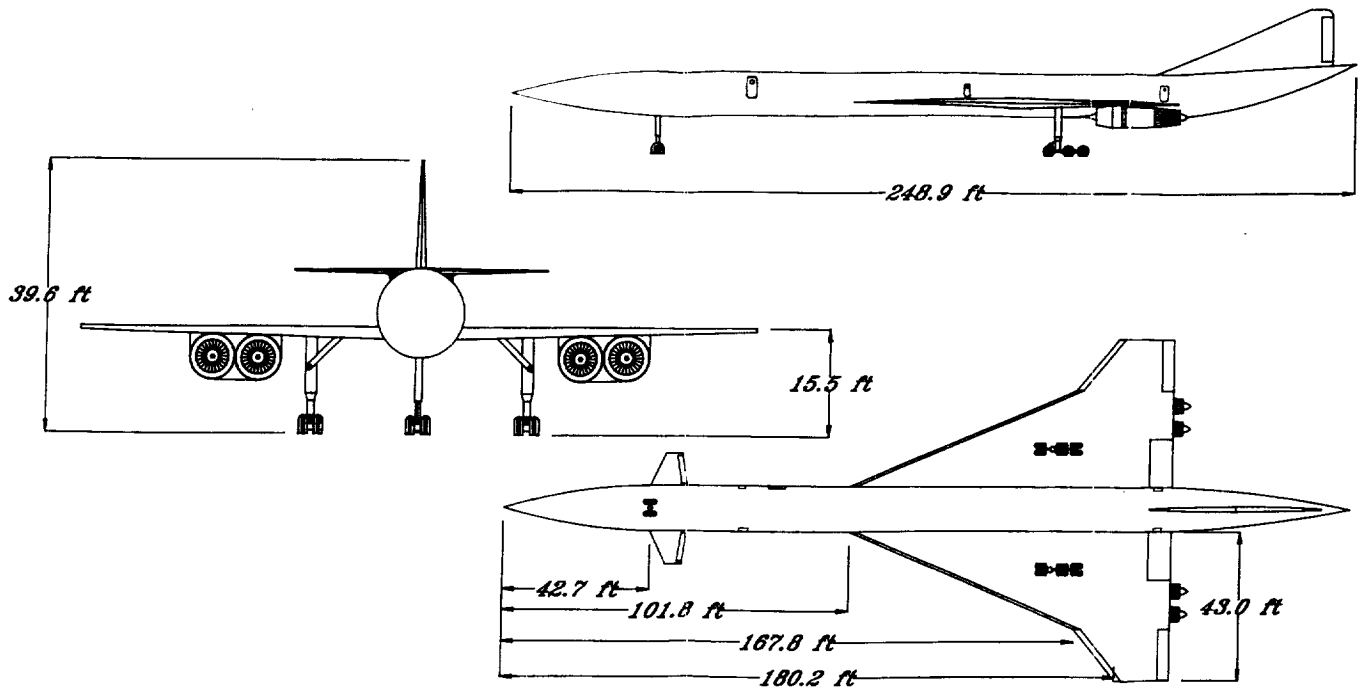
The market has never been better for a HSCT. With air travel



expected to increase greatly in the next ten years, the Phoenix can expect to see a production run of several hundred aircraft. This will breathe new life into an American aircraft industry that has seen a slight drop in its worldwide dominance. The Phoenix is the aircraft of the future! Figure 1.0.1 shows the final three-view of the Phoenix.

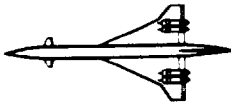
# Phoenix

Figure 1.0.1 - Three View



4.





## 2.0 Mission Description

Phoenix is designed to carry 152 passengers with a mix of 90% business and 10% first class passengers along city-pair routes of 5150 nautical miles distance or less at a design cruise speed of Mach 2.5. The typical mission profile consists of seven distinct phases (see Figure 2.0.1).

1. Startup and taxi - The startup and taxi run are scheduled for 15 minutes duration. This phase begins with main engine start and ends when the takeoff roll commences.
2. Takeoff and climb - A maximum weight takeoff roll and initial climb to flight level 30 (30,000 feet mean sea level (MSL)) at subsonic speeds comprise this phase. Below flight level 10, maximum speed is restricted to 250 knots indicated. Between flight level 10 and flight level 30, flight speed is Mach 0.87.
3. Acceleration to cruise Mach - At 30,000 feet, Phoenix begins a five minute acceleration to Mach 2.5 begins. Minimum passenger level g-loads are limited to 0.85g during this phase.
4. Cruise - Phoenix cruises at Mach 2.5 at 60,000 feet. Cruise time for a mission distance of 5150 nautical miles is 2.7 hours.

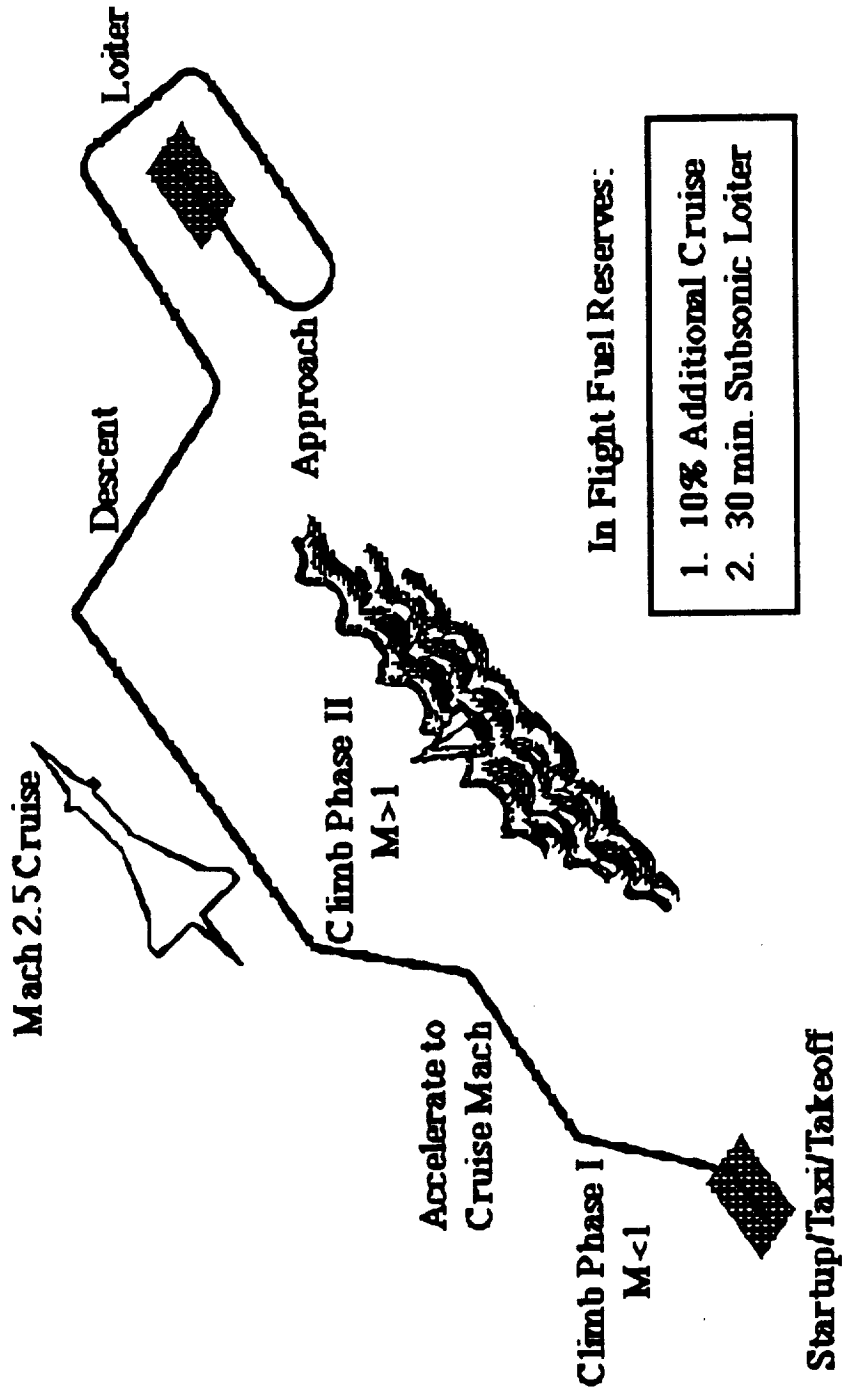
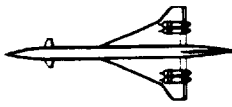
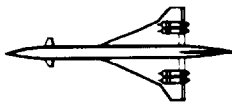


**Figure 2.0.1: Phoenix Mission Profile**

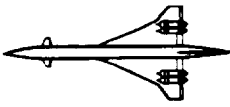


## *Phoenix*

5. Descent - Supersonic velocity is maintained down to flight level 30. At this altitude Phoenix decelerates to Mach 0.85. At flight level 10, the vehicle decelerates to 250 knots indicated. Descent phase ends at 1500 feet above ground level (AGL).
6. Approach and landing - A ten minute hold at 1500 feet AGL precedes approach and landing. Indicated velocity on approach is 158 knots.
7. Taxi-in and ramp dock - Eight minutes is allotted for this phase of flight.

Fuel reserves for the vehicle include enough fuel for an additional 10% of route distance at cruise Mach followed by 30 minutes of subsonic loiter at 1500 feet AGL.

Supersonic flight over land is not considered feasible and was not incorporated into the vehicle design. This is due to low public tolerances for sonic booms. All overland flight will be conducted at high subsonic Mach numbers. According to the Carlson N-wave equation of Reference 1, N-wave overpressure levels during supersonic cruise do not exceed 2.1 psf for straight and level flight.



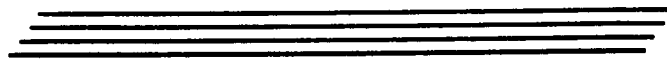
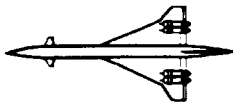
### 3.0 Preliminary Sizing

In order to begin the design process, a baseline estimate of the takeoff weight of the aircraft was necessary to determine the wing planform size and propulsion requirements. The iterative fuel fraction method outlined in Reference 2 was employed, using the mission parameters and performance assumptions shown in Table 3.0.1.

**Table 3.0.1: Mission Parameters**

Mission Range (n.m.)	4700
Passengers	150
Weight/Passenger (lbs)	210
Crew	7
Weight per Crew (lbs)	200
Cruise TSFC (lbs/lbs/hr)	1.17
Cruise L/D	9.5
Loiter TSFC (lbs/lbs/hr)	0.77
Loiter L/D	9

Due to the prediction of a large increase in passenger traffic in the Pacific Rim, an initial range of 4700 nautical miles was chosen to exploit this expanding market. By holding this range constant, the capacity of the aircraft was then varied to determine the configuration that yielded the maximum revenue, based on the predictions of Reference 3. The thrust specific fuel consumption (TSFC) and lift to drag ratios were



chosen based on existing technology and previous HSCT trade studies (Reference 4).

The class one sizing performed for Phoenix indicated a gross takeoff weight of 620,000 lbs with a mission fuel weight of nearly 325,000 lbs. Initial sizing also indicated that takeoff performance was driving the needed thrust-to-weight ratio. Cruise thrust was well below the thrust required for one engine inoperative (OEI) takeoff. The propulsion plant selected for the vehicle allows unaugmented supercruise. No other phases of flight were thrust critical. FAR 25 OEI takeoff requirements for Phoenix stipulate an obstacle clearance of 35 feet at the runway end. This requirement set the class one thrust-to-weight ratio for Phoenix. at 0.4.

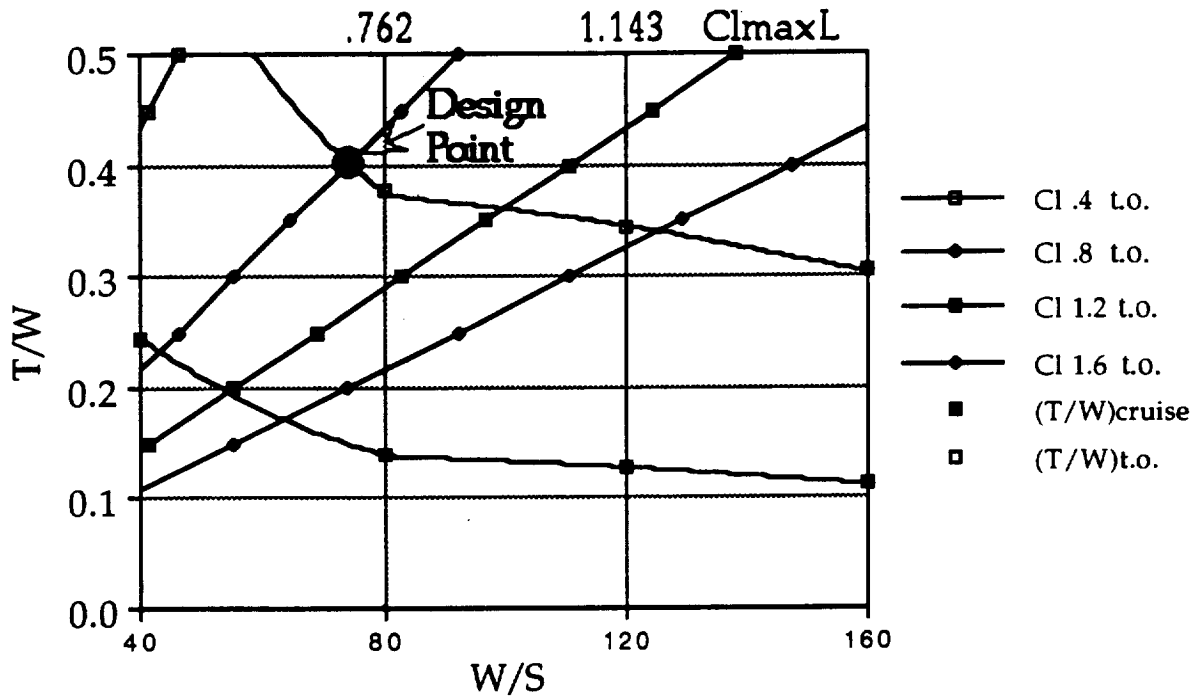
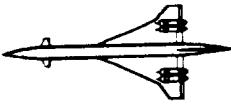


Figure 3.0.1: Sizing Matrix Plot



# Phoenix

Takeoff constraints determined the required wing loading as well. The velocity required to achieve sufficient lift for flight was excessive for wing loadings higher than 95 psf. The class one design point selected for Phoenix is shown in Figure 3.0.1. This point requires a thrust-to-weight ratio of 0.40 and a wing loading of 72 psf. Class two design reduced the thrust-to-weight ratio to 0.33 and increased the wing loading to 83 psf.

The first cut takeoff weight of 650,000 lbs seemed excessive when compared to other transport aircraft with comparable payload and range. Class two sizing was centered around an attempt to reduce the gross takeoff weight to a value closer to 450,000 lbs. Table 3.0.2 depicts the sensitivity of the initial gross takeoff weight to various parameters. The sensitivities indicated that optimization centered around the fuel load would yield significant reductions in weight. The reduction in thrust-to-weight ratio mentioned above, coupled with a reduction in TSFC and an assumption of 10% reduction in structural weight accounted for most of the reduction to the final weight for Phoenix. The reduction in TSFC was realized through careful engine selection. The reduction in structural weight was assumed reasonable because of increases in the level of structural technology and the use of composites where applicable.

Final takeoff weight for Phoenix was reduced to 455,000 lbs. This weight was confirmed using three separate tools: the initial sizing tool, the weight and balance calculations, and the mission performance integration program.

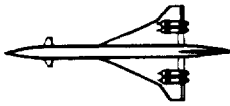


**Table 3.0.2: Gross Takeoff Weight Sensitivities**

Payload Weight (lbs/lbs)	12.4
Empty Weight (lbs/lbs)	2.3
Cruise Range (lbs/n.m.)	287
Loiter Time (lbs/hr)	285940
Cruise Velocity (lbs/kt)	-.2
Cruise TSFC (lbf/lbm/lbf/hr)	1,222,598
Loiter TSFC (lbf/lbm/lbf/hr)	185,675
Cruise L/D (lbs)	-150,572
Loiter L/D (lbs)	-20,630

Class two performance sizing was accomplished by integrating all aspects of the mission profile with respect to time. These integrations were performed by a computer and considered only along the longitudinal axis. No account was made for head or tail winds during flight. The parameters which resulted from the sizing are listed in Table 3.0.3

**Table 3.0.3: Final Sizing Results**

M <sub>cruise</sub>	2.5	Range (n.m.)	5150
Passengers	150	S <sub>ref</sub> (sq. ft.)	5490
W <sub>fuel</sub> (lbs)	209,950	W <sub>takeoff</sub> (lbs)	455,000
W/S	83	T/W	.33

## 4.0 Configuration

### 4.1 Fuselage Configuration

The fuselage consists of a circular double wall configuration. This design was used to provide a fail-safe fuselage structure that would allow enough protection to the passengers and crew inside should the hull integrity be breached. If pressure is lost, the difference in pressure would cause catastrophic physiological damage and adequate time for the aircraft to reach a safe pressure altitude would be a significant problem at 60,000 feet. Both fuselage shells are designed to withstand a pressurization of 15,000 feet at the designed cruising altitude of 60,000 feet. The resulting shell thickness is 9 inches, consisting of a 0.16 inch thickness for each shell skin, 3 inches for spar spacing, 5 inches for insulation, and the remaining space for all panels and dividers in the fuselage wall as shown in Figure 4.1.1.

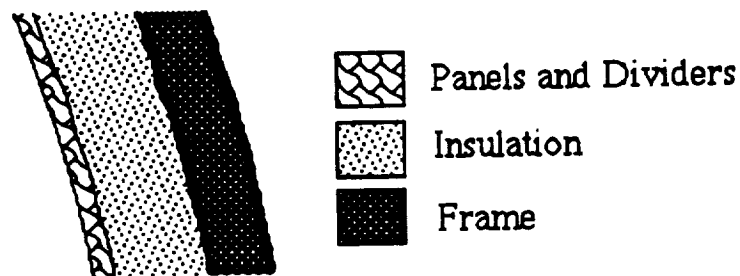
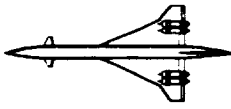


**Figure 4.1.1: Structural Cutaway**

Fuselage wall integrity is enhanced by not incorporating windows into the passenger section. In order to maintain a fail-safe





design, construction of windows would present a significant engineering problem. Either two windows would be needed or some other fail-safe design to maintain the double-hull integrity. In addition, structural considerations need to consider the extreme pressure differences incurred during each cycle. By incorporating windows, the aircraft would pay a significant weight penalty. Personal video screens will substitute the use of windows for the passengers and offer the option of showing various user selectable outside views.

The resulting fuselage configuration consists of a length of 249 and a wing span of 99 feet . The fineness ratio of the aircraft is 0.055 . A Von Karman nose is used to help minimize wave drag. Due to the nose length being 43 feet long, visibility is greatly reduced. For structural and weight considerations, the nose will not mechanically rotate to improve vision. Rather, vision requirements will be meet by use of synthetic vision. The tail is slightly upswept above the fuselage to help achieve the rotation angle.

The trade study determining fuselage configuration for Phoenix is provide in Table 4.1.1.

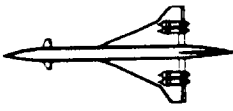
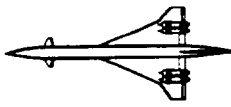


**Table 4.1.1: Fuselage Trade Study**

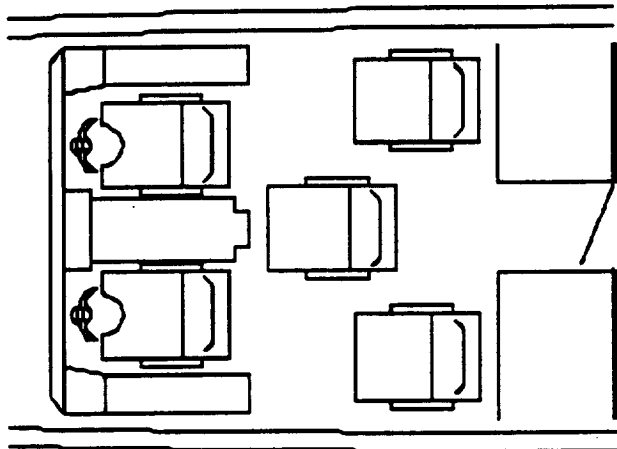
Shell	Advantages	Disadvantage
Single	Weight savings and access to routine service inspections	If rupture occurs, passengers and crew would be seriously injured. Not enough time would be allowed to safely reach acceptable pressure altitude.
Double	Fail-safe design provides additional safety	Weight penalty, more complicated to manufacture, and routine service inspections would be difficult to perform.
Circular	Even distribution of pressure, requires standard manufacturing techniques.	Smaller cross-sectional area for a fixed minimum radius.
Oval	Greater cross-sectional area, more area for structure, landing gear, fuel and passenger convenience.	Difficult to manufacture, requiring special tooling, and higher stress loads on shell due to pressure loading.



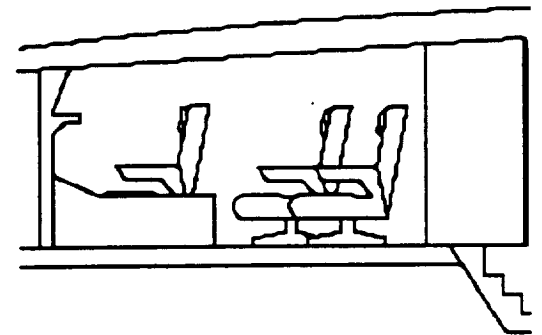
## 4.2 Flight Deck

The flight deck is designed to accommodate two flight officers and two observers. Due to the automation of the aviation and flight control systems, two flight officers are sufficient for operation.

Figure 4.2.1 shows the flight deck layout. Due to the special nose design with its limited visibility, synthetic vision will be incorporated into the avionics to provide improved visibility over the nose and in bad weather.



Flight Deck Plan View

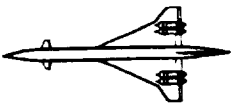


Flight Deck Elevation View

**Figure 4.2.1: Flight Deck Configuration**

## 4.3 Interior Layout

The fuselage is designed to comfortably accommodate 152 passengers. First class accommodations, shown in Figure 4.3.1 consisting of 10% of the passenger layout, are located in the forward section of the fuselage. The remaining 90% is business class, shown in Figure 4.3.2 divided into two sections and located aft of the main



loading door. A 10% first class and 90% business class split was selected to achieve a comfortable aircraft that would be primarily directed to those passengers whose time is of importance. No economy class was included in the design. The anticipated price of a ticket on the Phoenix is prohibitive for most tourists. The time of the first class and business traveller is valuable enough to warrant paying the surcharge for supersonic flights.

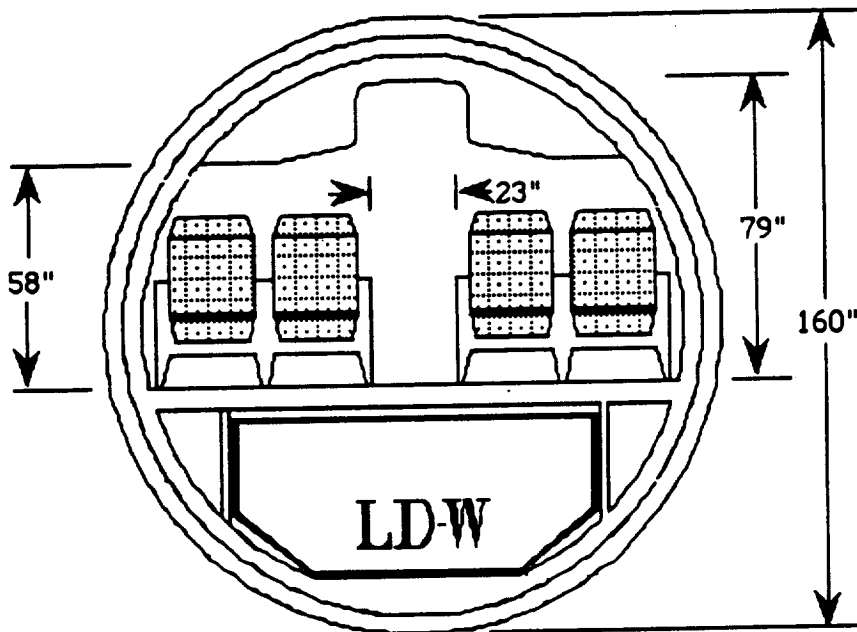
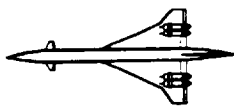


**Figure 4.3.1: First Class Cross Section**

One design consideration was to incorporate a comfortable environment for the passengers to work or rest in peace. All seats will have modern conveniences of personal air phones and video displays, which will allow the passenger to choose between business, entertainment, or outside viewing functions. Approximately 30



passengers are allotted per flight attendant. First class accommodations include wardrobes, a lavatory and a separate galley. Business class accommodations include wardrobes, four lavatories and two galleys. Seat dimensions for the two classes are shown in Table 4.3.1. For cargo loading compatibility, the belly of the fuselage is able to accommodate LD-W containers.

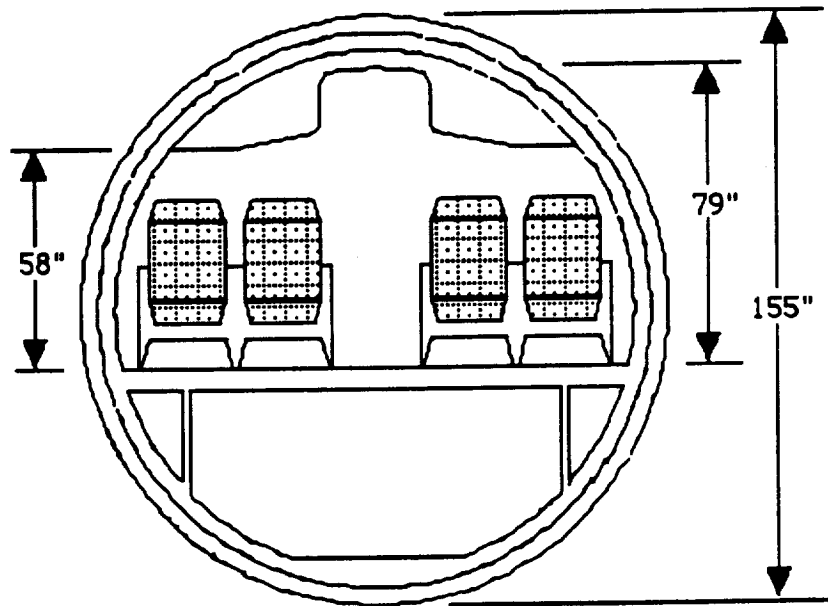


**Figure 4.3.2: Business Class Cross Section**

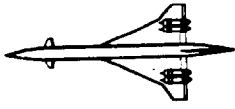


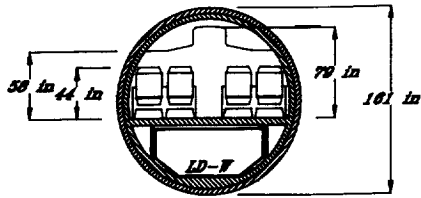
**Table 4.3.1: Seat Dimensions**

Class	First Class	Business
Seating Configuration	2 by 2	2 by 2
Seat Pitch	48"	36"
Seat Width	22"	20"
Seat Height	44"	44"
Aisle Width	23"	23"

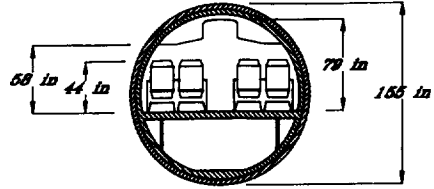
The detailed inboard layout is shown in foldout Figure 4.3.3.

# PHOENIX

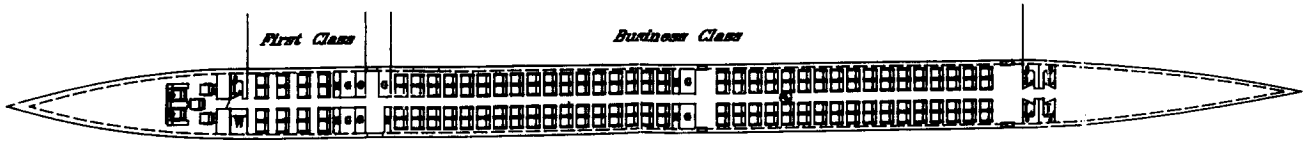
Figure 4.3.3 - Inboard Layout



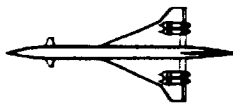
First Class



Business Class



G - Galley  
L - Lavatory  
W - Wardrobe



#### 4.4 Wing Design

Due to the greatly varying flight regimes of a supersonic transport, the design of the wing planform of Phoenix was a study in compromise. Subsonic flight is optimized by a high aspect ratio wing with a smooth leading edge and moderate thickness. Conversely, during supersonic cruise the large forces produced by the high dynamic pressure warrant a small planform with highly swept leading edges to minimize the component of flow perpendicular to the leading edge. Additionally, the wing should be thin with sharp leading edges to minimize wave drag.

Since the majority of Phoenix's mission profile is supersonic cruise, it was deemed necessary to optimize the planform for cruise. According to the preliminary weight sizing, the sensitivity of takeoff weight to cruise L/D was approximately -150,000 lbs (i.e. an increase in L/D of 1 would decrease the takeoff weight 150,000 lbs). Since low values of the lift coefficient are necessary in cruise, the magnitude of induced drag is decreased and wave drag and parasite drag become the major drag components. For the wing planform, wave drag is a function of the flow velocity component perpendicular to the leading edge. A major reduction in wave drag is achieved if the leading edge is swept greater than the mach angle ( $\sin^{-1}[1/M]$ ), so that the flow over the leading edge is subsonic. Figure 4.4.1 shows the chordwise flow velocity.



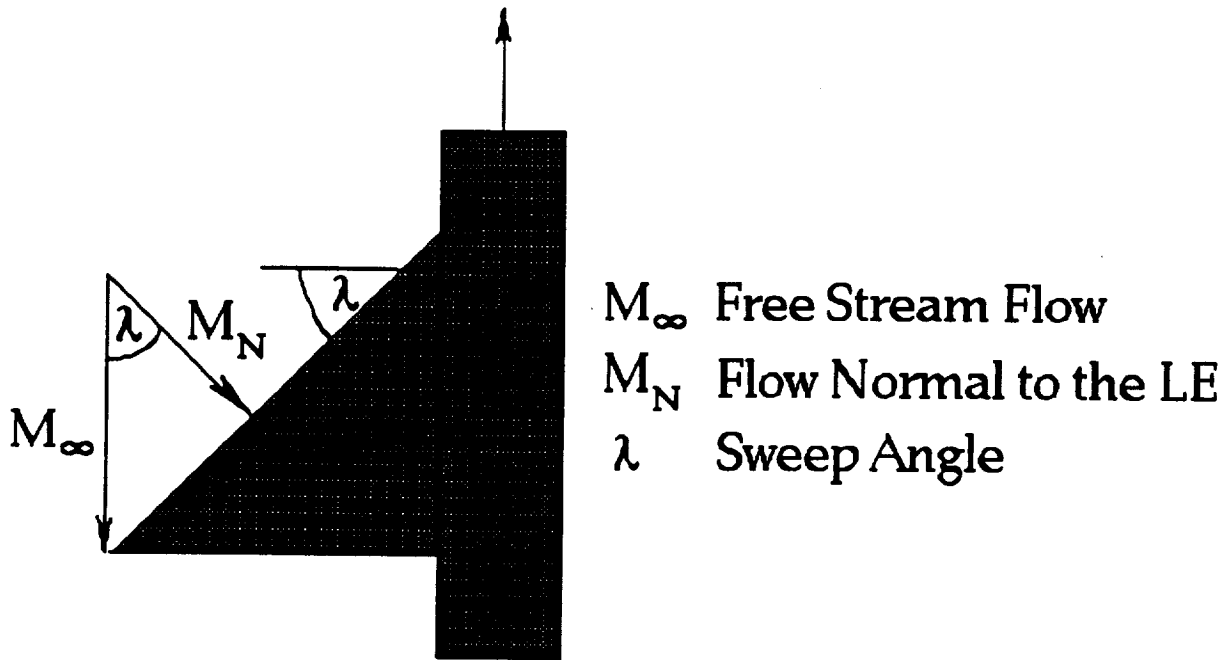


**Figure 4.4.1: Chordwise Flow Velocity**

Therefore, for a design mach number of 2.5, wave drag would be optimized by a delta wing with a leading edge sweep of at least  $64.5^\circ$ . Additionally, with a subsonic leading edge a subsonic airfoil with a larger thickness may be used. A larger thickness lowers the structural weight and increases the volume that can be used for fuel storage. Although a straight delta wing is optimum for supersonic flight, the subsonic performance is poor. Because of the large sweep of the leading edge, flow over a delta wing is dominated by vortex flow on the top surface of the wing. The vortices formed at the leading edge of a delta wing are formed the same way that wing tip vortices are formed on a rectangular planform. They coalesce over the top surface into two distinct vortices that are responsible for the majority of suction on the top surface. Unfortunately, the escape of air to the top surface reduces the

pressure on the bottom surface that contributes to lift. Consequently, delta wings have very shallow lift curves. Figure 4.4.2 shows the planform geometry candidates that were considered.

A trade study was conducted (Table 4.4.1) to choose a planform that offered a compromise between subsonic and supersonic performance.

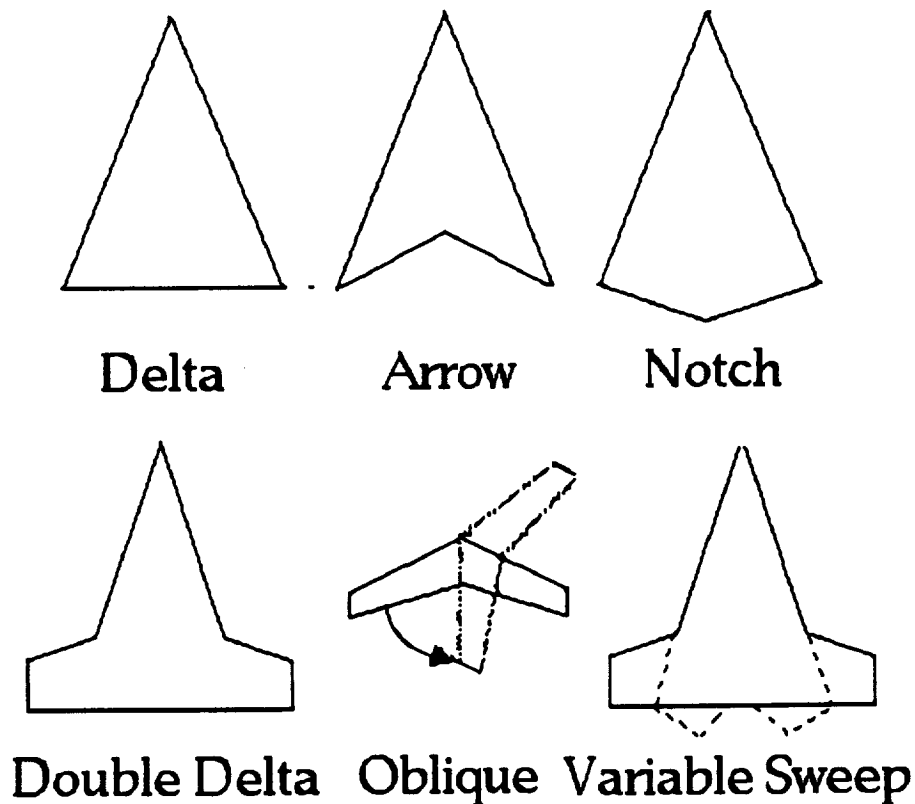
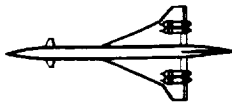


**Figure 4.4.2: Planform Geometry Candidates**

Although a double delta is more difficult to manufacture than a delta wing with an unbroken leading edge, it offers several advantages. First, by decreasing the sweep angle of the outboard section, the wing span is increased. Since aspect ratio is a function of span squared, induced drag

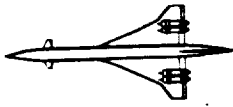


is reduced. Second, the rearward shift in the aerodynamic center between subsonic and supersonic flight is reduced with a larger aft delta. Third, the reduced sweep of the second delta contributes positively to the lift slope. Finally, the double delta configuration has been used successfully and there is a relatively large database of information on these planforms.

Although not as influential as the sweep of the leading edge, the disposition of the trailing edge is also a design factor. Delta wing planforms with a notch in the trailing edge, called arrow wings, or those with an added triangular area, called diamond wings, offer improvements over the standard trailing edge but mainly at high angles of attack. Since a commercial transport will rarely operate at high angles of attack, and a straight trailing edge is more amenable to manufacturing, these planforms were discarded.

A derivative of the delta wing planform, variable sweep delta wings were considered early in the preliminary design phase. The potential advantage of having a large planform at takeoff that retracted within the mach cone for supersonic cruise is offset by the large weight penalty for the hinge mechanism. Placement of the hinge is also critical, considering the small wing thickness allowed for supersonic flight.

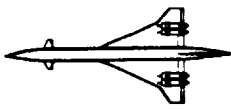
The last design configuration considered was an oblique wing. Due to the ability to rotate the whole planform, the supersonic drag is reduced so that very high cruise L/D values are attainable. Like the swing wing, this configuration also suffers a weight penalty for the hinge mechanism to rotate the wing. In addition, the lack of a large database of



experimental data deemed this configuration beyond the scope of a year-long design.

**Table 4.4.1: Wing Trade Study**

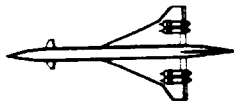
<b>Wing Type</b>	<b>Advantages</b>	<b>Disadvantages</b>
Delta	Easier to manufacture Lower wave drag	Low C.L.alpha Large C.G. shift
Double Delta	Better lift slope Smaller C.G. travel Larger aspect ratio	Harder to manufacture
Cranked Delta --Arrow Wing --Diamond Wing	Slightly better lift slope than double delta Better high angle of attack characteristics	Straight trailing edge is better for structural and manufacturing considerations
Variable Sweep	Higher C.L. at takeoff Smaller wing area in supersonic cruise	Weight penalty for pivot Thin wing makes pivot placement difficult
Oblique Wing	Lowest drag in supersonic flight Best L/D	Large research and development costs Large weight penalty for pivot Pivot is in center of passenger compartment



Because of the large wave drag penalty associated with leading edges with a small degree of sweep, it was decided to pursue a delta wing configuration. In order to improve the subsonic characteristics of the wing, the chosen planform is a double delta wing with the outboard section having a supersonic leading edge. Because of the manufacturing penalties of arrow and notched trailing edge configurations, the trailing edge is straight.

#### **4.5 Empennage Design**

In consideration of longitudinal and lateral-directional control, a trade study was performed for two possible configurations to make for such allowance. A brief summary of the study for a horizontal/vertical tail and a canard/vertical tail configuration are presented in Table 4.5.1 which shows some basic advantages and disadvantages associated with each configuration. Disadvantages outweigh benefits for many of the uses of a canard. Negative wing-canard vortex interactions can ruin lift development by the wing. Additional structural considerations need to be made for the integration of canards in a configuration. Such allowance reflects in increased weight. Although canards can provide controllability in high-alpha attitudes, this aircraft is restrictive in the angle of attack flown. However, the negative aspects of canard use can be superseded by benefits if the basic limitations of canards are recognized and a fly-by-wire system is put to use. Canards should not be expected to be major load carriers. Wings are better suited for

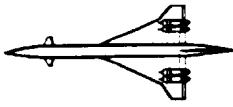


higher loadings given the greater area. Canards can be used for developing substantial moments when given adequate moment arms to function about.

**Table 4.5.1: Empennage Trade Study**

<b>Configuration</b>	<b>Advantages</b>	<b>Disadvantages</b>
Horizontal and vertical tail	Large database Conventional	Trim drag penalty Large area and corresponding drag Tail download must be overcome by wing lift
Canard and vertical tail	Lower trim drag Very effective for achieving rotation at liftoff Positive upload = lift	Possible destructive vortex interaction with wing Complex analysis

For take-off purposes, a horizontal/vertical tail and canard/vertical tail configuration were considered as candidates in the Phoenix design. The horizontal tail is as functional as a canard in regard to longitudinal control. For the horizontal tail to be most effective, the a.c. needs to be distant from the tail location. Since the aerodynamic center is usually constrained toward the back end of an aircraft for



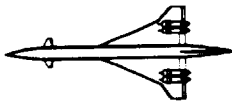
rotation requirements, the horizontal tail must be large to compensate for the reduced lever arm. Large areas on a supersonic transport translate into large wave drag problems. The use of a canard in this case would prove most beneficial. Since the canard can be located toward the front end of an aircraft, a larger lever arm is available and the consequent size of the canard can be greatly reduced. A disadvantage of the canard not experienced by the horizontal tail is the wing-canard vortex interaction. The nature of this interaction is and may likely detract from the lift development of the wing. However, the relatively small canard disposition is expected to lessen this effect and serve more as a benefit than a detriment.

Regarding weight concerns and associated costs, the canard is a better contender than the horizontal tail. The smaller size of the canard permits for lessened weight and cost. Structural concerns for both the canard and horizontal tail are similar, yet the integration of the canard must be more carefully planned so not to interfere with traffic in the section of fuselage attachment is made.

The particular configuration of Phoenix due to supersonic regards and the continual concerns of weight and cost savings dictate that the canard/vertical tail is better suited for this design than the horizontal/vertical tail configuration. In either case, the vertical tail is included to address lateral control needs.

#### **4.6 Engine Placement**

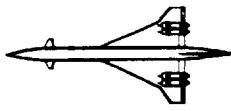
There are several considerations regarding engine placement.



## *Phoenix*

First, the engine must be placed somewhere where the aircraft can structurally carry the loads. Additionally, the engines must be placed somewhere where the airflow to the inlet will not be disturbed. Taking these two factors into account, the engines are placed on the wing. To carry the loads, the engines are attached to a structural spar. Mounting the engines on the fuselage requires exceptional structure rigidity which creates an additional weight penalty. For this reason, the engines are mounted on the bottom of the wing instead of the top because of the interference of the airflow into the inlet by the wing at high angles of attack. This is another reason for not mounting the engines on the fuselage. The engines were placed together in pairs because of the lack of mounting space on the underside of the wing. This placement is not affected by the landing gear which is located forward and off to the side of the engine inlet. Another reason for placing the engines under the wing is ease of maintenance. In this location, the access panels are within easy reach. Should the engine need to be removed, this is easily done by dropping it from its wing mount.





## 5.0 Aerodynamics

### 5.1 Fuselage Aerodynamics

To help reduce interference drag, components of the fuselage have been tailored. Small fillets are located between the fuselage and canard. In addition, the wings are blended into the fuselage body. In order to reduce the base drag produced by aft facing surfaces, the upsweep angle of the fuselage tail is set at  $8.5^\circ$ , and is gradually implemented in order to approximate an isentropic expansion. This value is constrained by the requirement that the tail does not scrape the runway at takeoff rotation.

Further modifications for drag reduction include area ruling along the length of the fuselage where a minimum diameter of 155 inches is reached compared to the maximum diameter of 161 inches. Theoretically, the minimum wave drag at Mach 1 is achieved by a body with an internal volume distribution that minimizes curvature longitudinally (Reference 5). As the Mach number exceeds one, the volume distribution is determined by intersecting the volume with planes set at the Mach angle ( $\sin^{-1}[1/M]$ ) relative to the free stream. The volume distribution for each station is the average of the volumes about different roll angles. Because of the complexity of this calculation, the Phoenix fuselage was area-ruled in the longitudinal axis only. The equivalent body of revolution is shown in Figure 5.1.1.

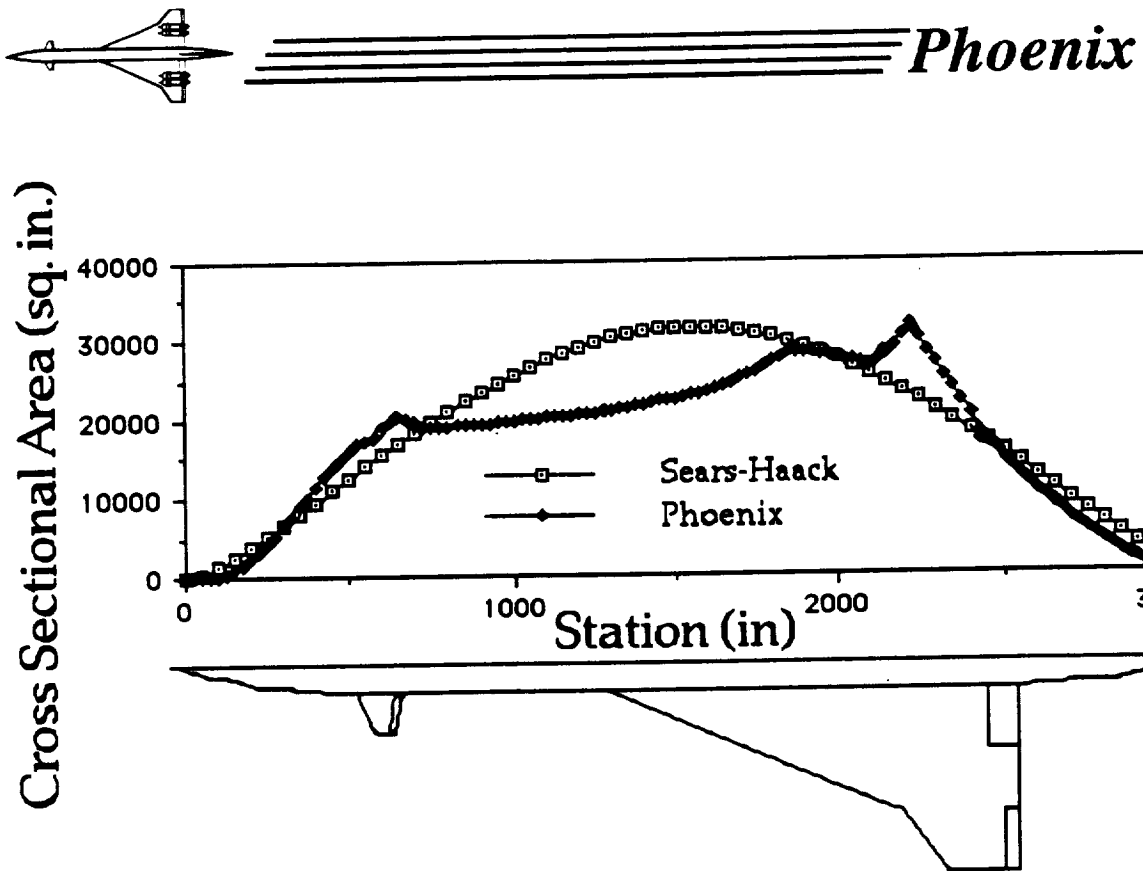
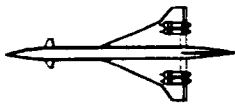


Figure 5.1.1: Phoenix Area Distribution

## 5.2 Wing Parameters

In the preliminary design of the wing, the maximum thickness was set at  $0.05c$ , and the inboard sweep was set at  $70^\circ$ . The wing thickness was chosen after determining the necessary internal volume for fuel storage. The inboard wing sweep was chosen to keep the wing within the Mach cone. After the preliminary drag polars had been completed, the inboard sweep was reduced  $3^\circ$  to  $67^\circ$  for better subsonic performance while keeping the leading edge subsonic. In order to increase aspect ratio and develop a higher lift coefficient, the outboard wing sweep was set at  $50^\circ$ . Cruise trim requirements necessitated a wing incidence angle of  $1^\circ$ . Further stability and control analysis will determine the final wing dihedral.

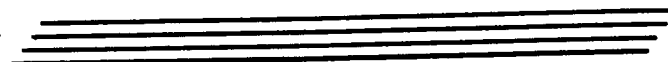
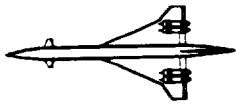


# Phoenix

Because the inboard wing section is swept inside the mach cone, a subsonic airfoil can be used. At the root of the wing, a NACA 64-209 airfoil was chosen. Several reasons drove this decision. First, the NACA 64-209 is a subsonic airfoil with a low thickness to chord ratio. Since decreasing the airfoil thickness increases the critical Mach number, the leading edge sweep can be decreased while still keeping the normal component of the free stream Mach number below critical number. The advantages of less leading edge sweep include lower structural weight and an increase in the lift curve slope. Additionally, the low thickness to chord ratio will facilitate the transition from a subsonic airfoil at the root to a supersonic airfoil at the tip. Finally, the NACA 64-209 has a relatively large leading edge radius, which is beneficial for the vortex flow that dominates the lift of a delta wing (Reference 8).

According to supersonic thin airfoil theory (Reference 7), minimum wave drag is achieved by minimizing the change in curvature of the surface with respect to the chord. For this reason, the airfoil chosen for the outboard wing section is a symmetric diamond. The airfoil sections between the root and the outboard break will be derivatives of the NACA 64-209 in order to achieve a smooth transition between the subsonic and supersonic airfoils. Because of the highly complex flow patterns over a delta wing, further aerodynamic tailoring is necessary in order to optimize the airfoil performance in both subsonic and supersonic cruise.

The final planform sizing was constrained by the performance sizing at takeoff. With the total runway length of 11,000 feet and a



rotation velocity of 181 knots, the thrust-to-weight and wing loading were iterated successively in order to minimize thrust required at takeoff for noise restraints (hence a larger planform) and to minimize the supersonic drag (small planform). Figure 5.2.1 shows the geometry of the wing. Table 5.2.1 summarizes the final wing parameters.

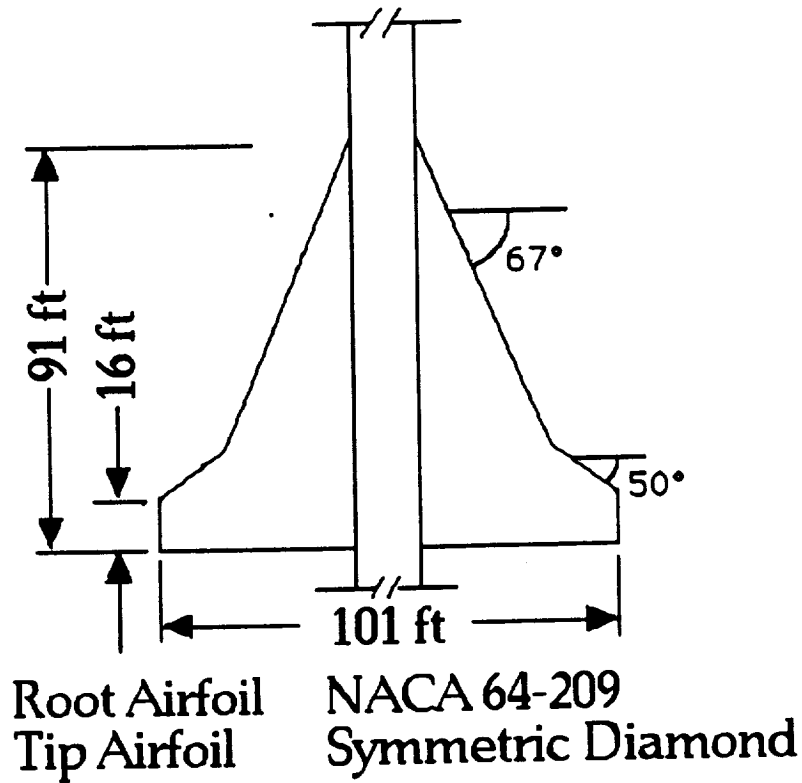


**Figure 5.2.1: Wing Geometry**

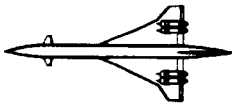
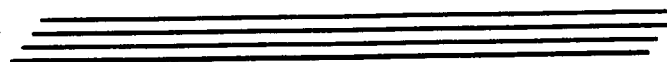
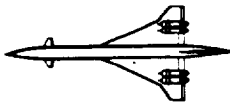


**Table 5.2.1: Wing Parameters**

Aspect ratio	1.84
Inboard Sweep Angle	67°
Outboard Sweep Angle	50°
Reference Area	5500 sq. ft.
Thickness Ratio	0.04
Root Chord	90 ft.
Wing Loading	83 psf

### 5.3 High Lift Devices

The choices for high lift devices on a delta wing are dictated by the vortices that develop on the upper surface of the wing. Figure 5.3.1 shows typical vortices formation on a double delta wing at a 10° angle of attack. The vortices develop near the leading edge, diverting slightly at the start of the outboard wing section. Experimental data indicates that high lift devices on the trailing edge in the vortex flow are less effective than in the axial flow inboard (Reference 6). Therefore, single slotted Fowler flaps are located on the inboard section of the wing. Although higher lift coefficients would be gained from double or triple slotted flaps, the benefits would be offset by the supersonic drag suffered due to the fairings necessary for the larger flap mechanisms. Since the flaps are located on the inboard section of the wing, flap mechanisms can be integrated in the wing-body blending. The flaps were initially sized due to the geometry restraints necessitated by engine placement, and subsequent analysis using LinAir, an inviscid vortex panel program. The



program indicated that sufficient lift augmentation is provided.

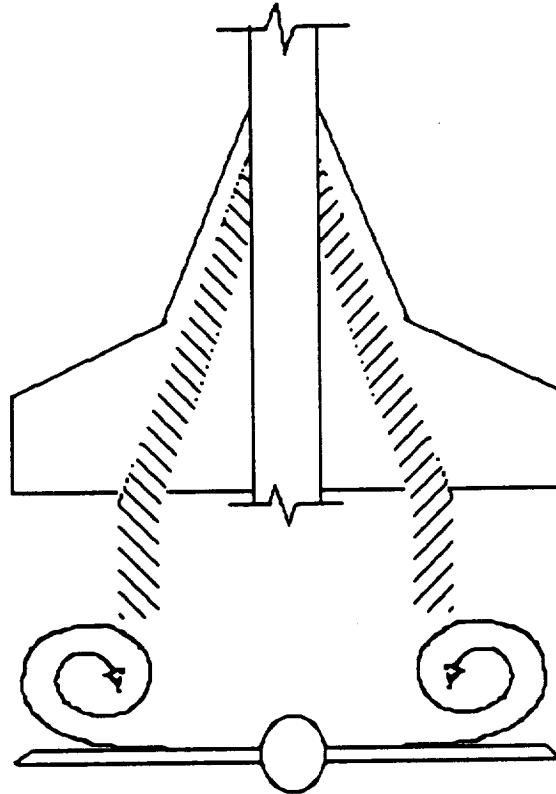


**Figure 5.3.1: Typical Vortices Formation**

On the leading edge, several high lift devices were considered as shown in Figure 5.3.2. Wind tunnel tests have been performed on several configurations (Reference 8), including the use of flaps, slats, or a leading edge gate as shown in Figure 5.3.2.

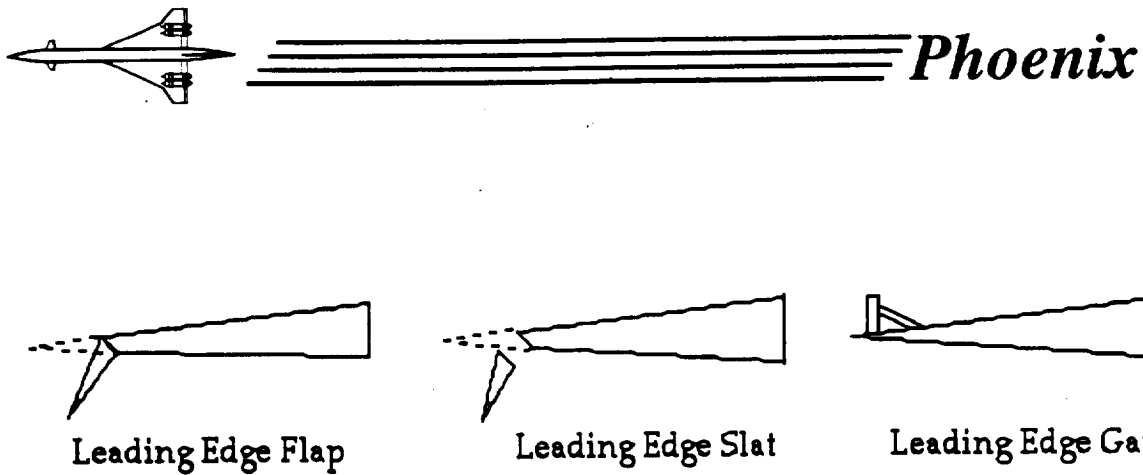
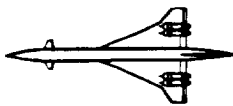


**Figure 5.3.2: Leading Edge High Lift Devices**

Slats are beneficial by allowing high pressure lower surface air to pass to the upper surface. This configuration was dropped because of the difficulty in fitting the mechanism in the restricted space in the leading edge without paying a substantial drag penalty for the mechanism fairing. Theoretically, the optimum lift to drag ratio for a delta wing is achieved with rounded leading edges. Wind tunnel tests have verified that leading edge flaps improve the lift coefficient by increasing the effective leading edge radius (Reference 6). The leading edge gate is based on the theory that gates add more high energy flow to the upper surface vortices without letting as much air escape from the lower surface. Since the leading edge flap and gate had less complex mechanisms than the leading edge slat, they were both retained for analysis using LinAir. The leading edge gate provided a total wing body  $C_L$  of .406, a 4% improvement over the leading edge flap, and was therefore retained for the Phoenix design. LinAir was also utilized to verify the conclusions of (Reference 8) that high lift devices are most effective across the entire leading edge.

Because of the shallow lift curve inherent in delta wing designs, the



leading edge gate will be used for lift augmentation during takeoff and initial climb under 10,000 feet AGL, as well as during approach and landing. During supersonic flight, the low lift coefficients necessary do not require the use of the gates. Table 5.3.1 summarizes the high lift devices on the Phoenix.

**Table 5.3.1: High Lift Device Parameters**

	Leading Edge Gate	Trailing Edge Flaps
S <sub>flap</sub>	87.8 sq. ft.	99.0 sq. ft.
b <sub>flap</sub> /b <sub>wing</sub>	1.0	0.27
d <sub>takeoff</sub>	90°	40°
d <sub>landing/approach</sub>	90°	60°

#### 5.4 Control Surface Sizing

Preliminary control surface sizing was made in consideration of controllability needs as well as fuel storage concerns and drag penalties. The smallest possible surface sizes were used to lessen the impact of wave drag during supersonic cruise. Small surfaces also allow for additional fuel storage space in the wings. Figure 5.4.1 illustrates the control surface arrangement used by Phoenix.



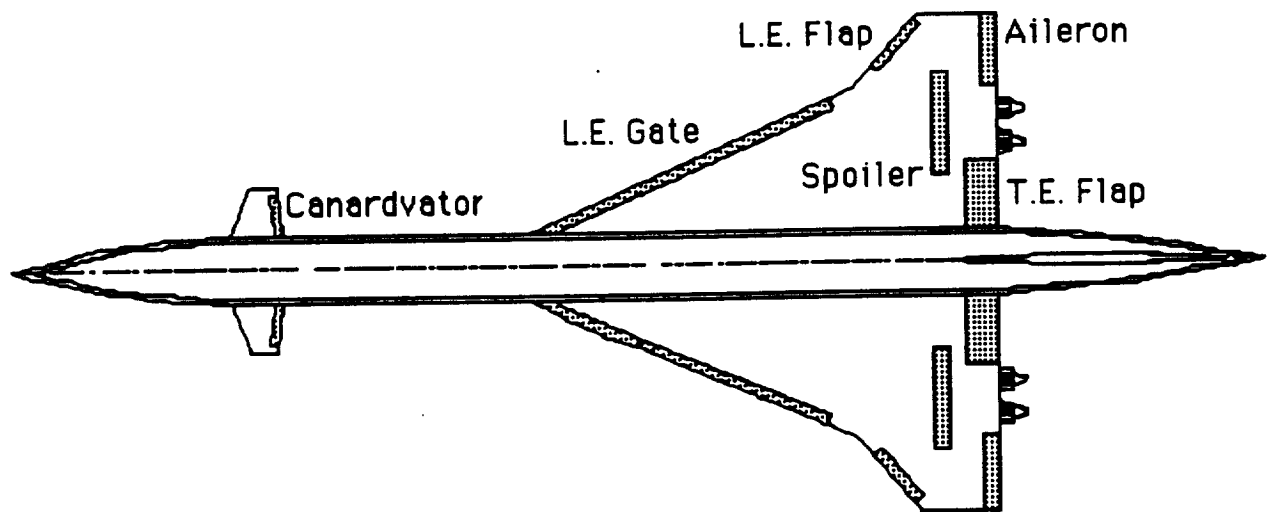
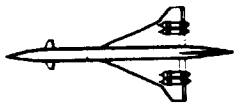


**Figure 5.4.1: Control Surface Arrangement**

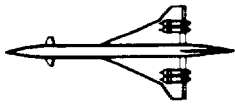
The use of leading edge gates predicted high enough benefits in lift to justify humble sizing of trailing edge flaps. The flaps serve mainly for longitudinal stability and control needs in concert with the canards. By careful arrangement of aircraft system and weight distributions, the aircraft's cg location is tailored near the aft portion of the aircraft for rotation purposes. The forward position of the canard from the aerodynamic center presents an idealized moment arm for both rotation and trim purposes. At no time is the canard relied upon for any major contribution to lift for the aircraft (refer to canard trade-study).

The sizing of the ailerons is done in recognition of their use for lateral control, namely to address roll-mode concerns. Since rapid roll maneuvers are not desired for this aircraft, large ailerons are not required. The low aspect wing configuration lessens the effectiveness of the ailerons by providing a reduced lever arm. However, the ailerons still need to be of adequate size and disposition to provide lateral stability and disturbance control. For this reason, the ailerons are placed



*Phoenix*

at extreme outboard location to make the greatest use of the lever arm available.



## **6.0 Drag Determination**

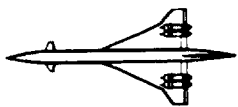
In order to verify the results of the initial takeoff weight sizing estimate, the assumptions about aerodynamic performance must be analyzed. The drag polars were calculated for takeoff, subsonic climb under 10,000 feet, subsonic cruise, and supersonic cruise.

### **6.1 Zero Lift Drag**

In order to compute the parasite drag for subsonic and supersonic flight, the wetted area was calculated for all the portions of Phoenix exposed to the free stream flow (Table 6.1.1). Engine inlet area was neglected in this analysis because the effects are included in installed engine performance. The drag due to the tail upsweep and flap deflection were calculated using the methods in (Reference 5). In addition, a 1% drag penalty was assessed for drag due to leaks and protuberances. It is assumed that careful attention to manufacturing detail and wing-body blending will justify this value.

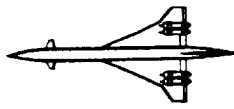
**Table 6.1.1: Component Wetted Areas**

Fuselage	10307 sq.ft.
Wing	8414 sq. ft.
Canards	490 sq. ft.
Vertical Tail	987 sq. ft.
Engines	2710 sq. ft.



## 6.2 Drag due to Lift

For subsonic flight, the induced drag was calculated using an estimate of 0.63 for the airplane efficiency factor, based on correlation with other swept wing aircraft. For supersonic flight, the efficiency factor was estimated using leading edge suction theory (Reference 5). On the outboard wing section the leading edge is supersonic and the induced drag term ( $k$ ) is assumed equal to the inverse of the supersonic lift slope ( $C_{di} = kC_l^2$ ). The supersonic lift slope for a diamond shape airfoil was estimated using TODOR, a program based supersonic thin airfoil theory. On the inboard panel, the leading edge suction was estimated as 30% based on calculations suggested by (Reference 5). Assuming a linear relationship between the efficiency factor and the radial distance from the fuselage, the supersonic induced drag term was estimated as 0.18. The calculation of the wave drag was estimated by comparing the cross sectional area of the Phoenix with a Sears-Haack body, which has the minimum wave drag for a closed-end body of the same length and total volume (Reference 5). This method is approximate, since it only compares the volume distribution perpendicular to the longitudinal axis, and does not account for the cross sectional area along the mach cone. More refined estimates are possible through existing computer codes such as the Harris Wave Drag Code, but were not available for our analysis.



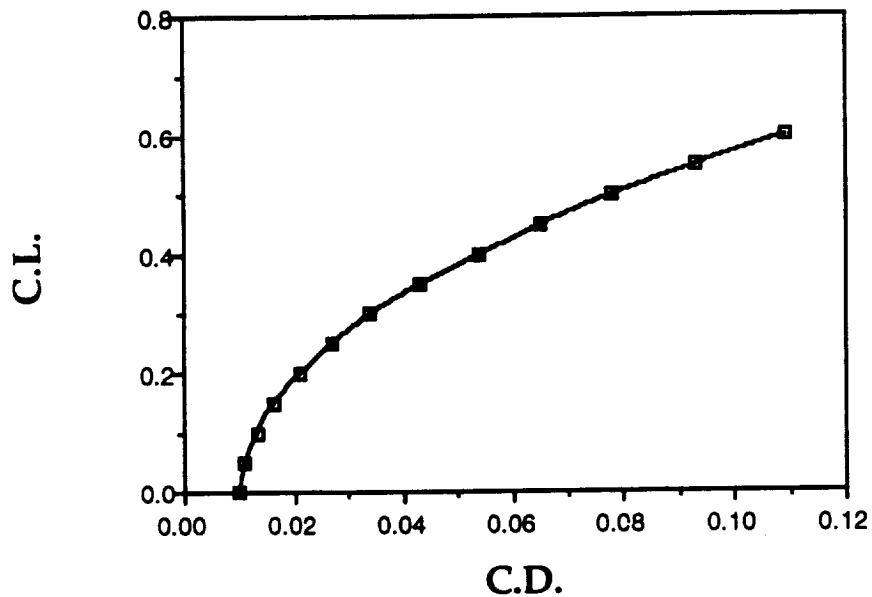
### 6.3 Lift to Drag Ratios

The drag characteristics of the Phoenix for various flight regimes are listed in Table 6.3.1. The maximum L/D was determined by intersecting the lift to drag curve with a tangent line drawn from the origin. The operating L/D was calculated by determining the lift coefficient necessary at that regime for steady unaccelerated flight.

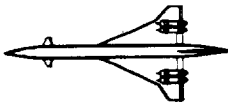
**Table 6.3.1: Drag Characteristics**

	Takeoff	Initial Climb	Subsonic Cruise	Supersonic Cruise	Landing
Max L/D	7.2	8.7	11.4	10.1	6.8
Operating L/D	4.6	7.9	9.2	8.6	3.9

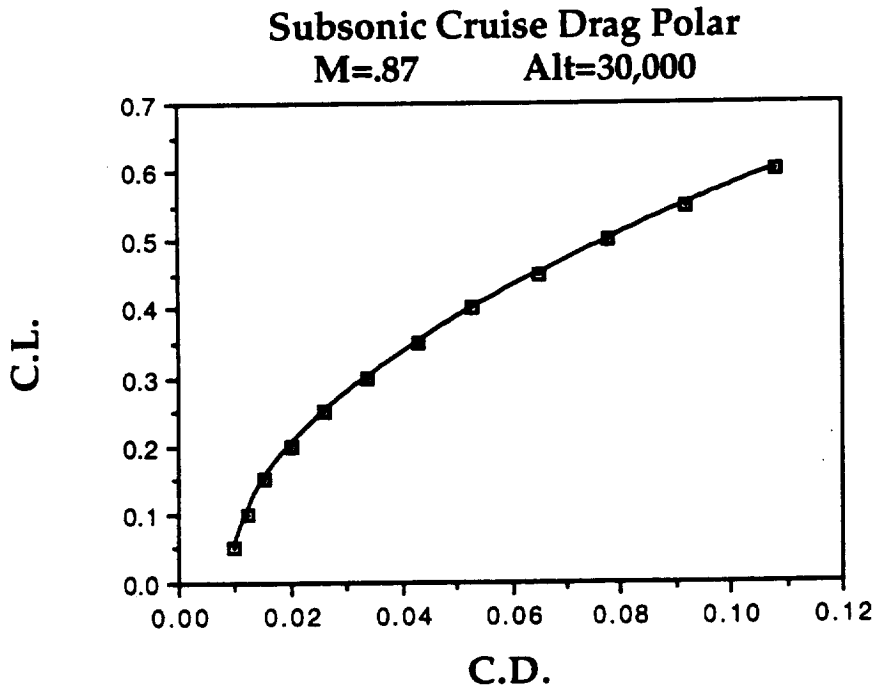
**Initial Climb Drag Polar**  
 V=250 kts Alt<10,000 ft



**Figure 6.3.1: Initial Climb Drag Polar**



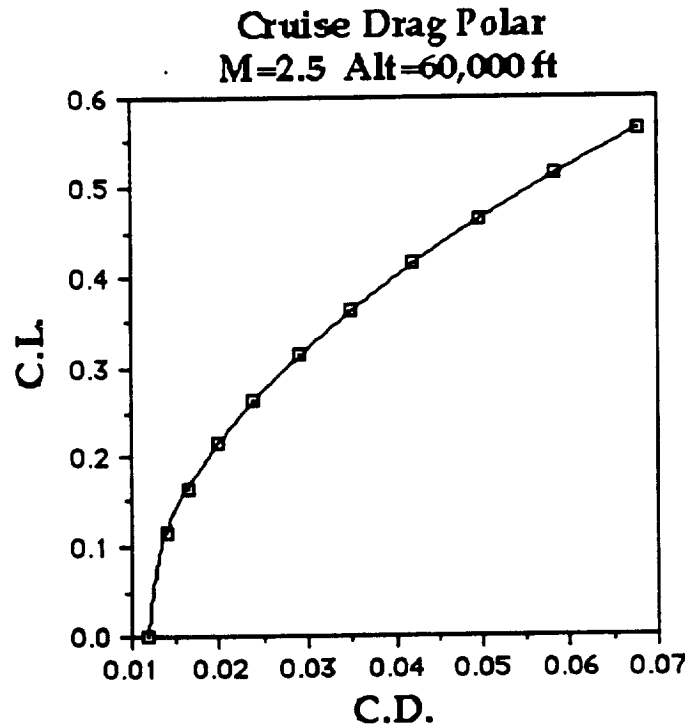
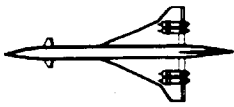
Figures 6.3.1 and 6.3.2 show the drag polars for the initial climb under 10,000 feet and subsonic cruise at a Mach number of 0.87, respectively.



**Figure 6.3.2: Subsonic Cruise Drag Polar**

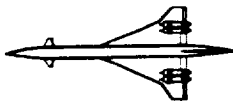
Comparing the subsonic drag polars to the L/D values used in the initial weight estimation, Figures 6.3.2 and 6.3.3 verify the previous performance assumptions.

Figure 6.3.4 shows the drag polar for supersonic flight. Based on this analysis the maximum lift to drag ratio is 10.1.



**Figure 6.3.3: Cruise Drag Polar**

Assuming the weight at the beginning of supersonic cruise to be 400,000 pounds, the lift to drag ratio at the lift coefficient necessary for level, unaccelerated cruise is 8.67. In order to meet the mission requirements, an 8% increase in the lift to drag ratio is necessary. With the wetted area of the planform set by takeoff constraints, the parasite drag is fairly constant and the method for increasing the L/D is decreasing the wave drag. Because of the approximate nature of the wave drag calculation and previous wind tunnel tests by Boeing and McDonnell Douglas that indicate L/D values in excess of 12 are possible, it is assumed that the use of wind tunnel tests and computational fluid dynamics could be utilized to optimize the area ruling and wing body blending to achieve the mission requirements.



## 7.0 Propulsion Integration

### 7.1 Selection of Engine

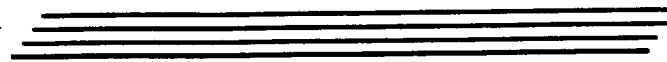
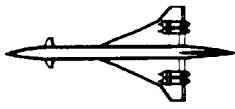
The engine selection was made using the design characteristics of the aircraft, which includes a takeoff weight of 455,000 pounds, a wing loading of 83 lbf/sq. ft., a cruise L/D of 9.5, and a thrust to weight ratio of .33. The engine that was chosen for the Phoenix was the NASA Mixed Flow Turbofan (MFT). The parameters of the NASA MFT engine are shown in Table 7.1.1 along with those of the baseline engine.

**Table 7.1.1: NASA MFT Characteristics**

	Unmodified	Modified
Takeoff Thrust (lbs)	52,000	39,000
Cruise Thrust (lbs)	16,774	12,600
Cruise TSFC (lbs/lbs-hr)	1.234	1.170
Loiter TSFC (lbs/lbs-hr)	.806	.770
Total Pod Length (lbs)	34.6	34.6
Total Pod Weight (lbs)	16,400	16,400

As will be discussed, the baseline engine is down-scaled in thrust to reduce the excess takeoff thrust. Takeoff thrust is the critical factor instead of the cruise thrust, so this is why the engine has excess cruise thrust. In addition to the thrust scaling, a 5% improvement is





made on the thrust specific fuel consumption (TSFC). This improvement is made so that the Phoenix weight becomes more manageable than what it would otherwise be. Figure 7.1.1 shows a mixed flow engine concept.

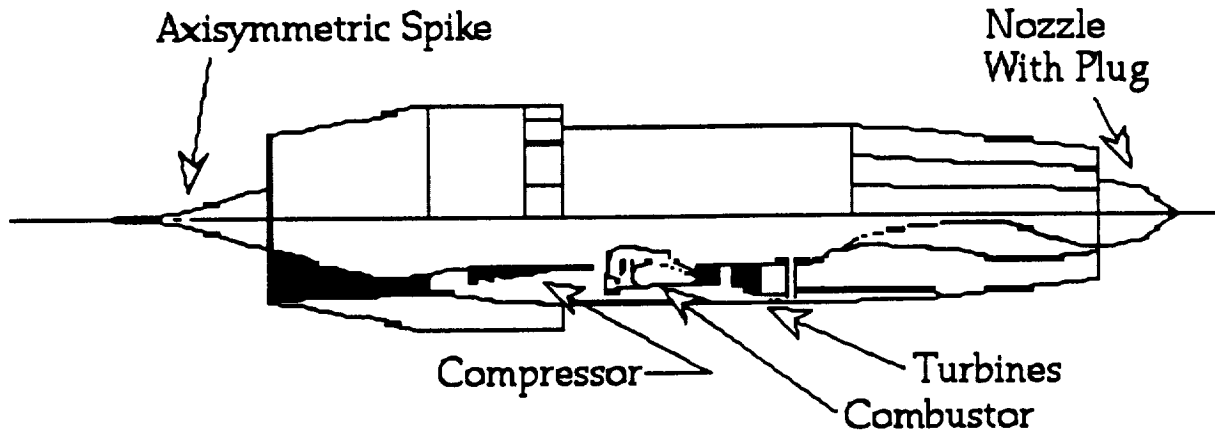
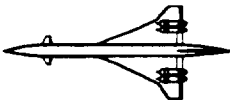


**Figure 7.1.1: Mixed Flow Turbofan Geometry**

To find an engine which would best suit the aircraft a trade study was conducted by examining five different engines. All of the engines studied were variations of low bypass turbofans. These engines were specifically targeted in the trade study because they can deliver the required performance necessary for a HSCT. Other engine types, such as high bypass turbofans and turbojets, are deficient in areas that are critical to an HSCT. High bypass turbofans can not operate at high speeds and turbojets have high TSFC's. For these reasons, only low bypass engines were considered. They were a supersonic through-flow fan (STFF), a Pratt and Whitney turbine bypass engine (TBE), a Rolls Royce tandem fan engine (TFE), and two different MFT's from NASA and General Electric. The trade study

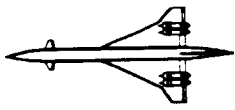


evaluated the five different engines on takeoff thrust, cruise thrust, cruise TSFC, loiter TSFC, and range. The results are shown in Table 7.1.2.

**Table 7.1.2: Engine Trade Study**

	Needed	STFF	NASA MFT	P&W TBE	RR TFE	GE MFT
Thrusttakeoff (lbs)	38,000	39,700	39,000	44,600	65,000	58,200
Thrustcruise (lbs)	10,500	13,600	12,600	10,700	8,500	10,600
TSFCcruise (lbs/lbs-hr)	Low	1.100	1.170	1.178	1.140	1.210
TSFCloiter (lbs/lbs-hr)	Low	.810	.770	.978	.855	.770
Range (n.m.)	5,100	5,439	5,150	4,978	5,223	4,985

In the evaluations, the characteristics for only one engine, out of the four required for this aircraft, was used. In order to keep this study impartial for all of the engines, the aircraft weight was held constant by varying the fuel weight. Using the information from the trade study plus the inherent qualities of the individual engines, the selection of an engine was made. The following paragraphs address the advantages and disadvantages of each engine.



### Rolls Royce Tandem Fan Engine:

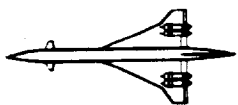
Of all of the engines being considered, this baseline engine is among the two that comes the closest to meeting Stage 3 noise requirements without the use of noise suppressers. The variable cycle design of this engine concept is what enables the engine to do this. Unfortunately, this same variable cycle design causes the engine to have very poor cruise thrust characteristics. This is the single biggest cause for its elimination. If this inherent design problem could be overcome, this engine would be a contender for Phoenix because of the good cruise TSFC.

### General Electric Mixed Flow Turbofan:

The baseline engine was thrust down-scaled by 5% because of the excessive thrust that it produced. Even so, the generation of 58,200 pounds of thrust at takeoff is substantially more than the 38,000 pounds needed. This means substantial increases for the cost of the engine and additional noise abatement problems. The engine can not be scaled down further because it already has just enough thrust for cruise. Of all the candidate engines, the General Electric engine has the highest cruise TSFC. Because of this, the range of the aircraft would not be maximized with this engine. For these reasons the GE engine was not selected for Phoenix.

### Supersonic Through-Flow Fan:

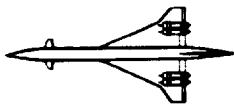
The baseline STFF engine had more thrust needed for both



takeoff and cruise. It also was designed to meet Stage 3 noise requirements (see Reference 9). The engine was down-scaled in thrust by 10% to lower the noise level an additional two to three decibels (see Reference 10). If an additional three decibels can be reduced, this engine will be able to meet Stage 4 noise requirements. This engine rates first for cruise TSFC and third for loiter TSFC, which makes it even more desirable. Although this engine appears to be a clear first choice for Phoenix, the technology for this engine will not be available for at least another twenty to thirty years; and that is assuming that a significant amount of time, resources and money is devoted to its development. If this engine type is developed and meets expectations, it will be a first choice for the Phoenix.

#### Pratt and Whitney Turbine Bypass:

The baseline engine was thrust down-scaled by 5 % to help assist in meeting the noise requirements and to reduce the excess thrust for takeoff and cruise. The areas that hurt this engine are the TSFC characteristics. For cruise this engine ranks fourth, however it is fairly close to the NASA MFT. The loiter TSFC is where this engine pays a big price. The associated range penalty is one of the worst for this higher loiter value. Because Phoenix has a high sensitivity to loiter TSFC, any time spent in loiter reduces the mission range. If this value can be lowered into the middle ranks, then this engine would be almost equal to the NASA mixed flow engine. Because it does not,



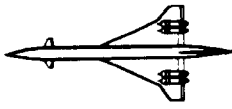
this engine is eliminated from consideration.

#### NASA Mixed Flow:

The baseline engine was thrust down-scaled by 25%. Doing this brings the thrust for takeoff very close to that which is needed, so there is not a lot of excess thrust. For cruise the engine ranks second for thrust output, and third for cruise TSFC. The loiter TSFC is the best among the five engines. Due to good performance characteristics of the NASA MFT and the poor performance characteristics of the others, the NASA MFT was chosen as the power plant for Phoenix.

### 7.2 Inlet Placement

The inlet for each engine is located directly in front of each of the engines. This may seem obvious, but there are other ways to place the inlets relative to the engine, such as an in the wing inlet. Deciding to place the inlets directly in front of the engines is based on simplicity and efficiency. From the standpoint of simplicity, the length of the inlet will be at its shortest in relation to other inlet configurations. This results in less space and weight taken up by the inlet. Maintenance and cost are additional factors that favor this inlet placement. From the perspective of efficiency, there will be fewer losses in directing the flow from the inlet to the engines. In deciding to place the inlet directly in front of the engine, placement of the engines becomes limited to the wing or fuselage.



### 7.3 Inlet Design

The inlet system is designed for Mach 2.5 and 60,000 feet. The type of inlet that is used for this engine is an axisymmetric spike that translates. Although this system is a little more complicated than a two-dimensional ramp inlet, it is lighter and has a better pressure recovery of about 1.5%.

### 7.4 Noise Requirements

Meeting the Far 36 Stage 3 noise requirements is a primary concern for engine selection. It has been suggested that Stage 4 noise requirements may be implemented, but the feeling in the aircraft industry is that meeting Stage 3 will be acceptable for now. Twelve decibels of suppression is achievable with 1990's technology (see Reference 8). This suppression will enable many engine concepts to meet Stage 3 requirements. The NASA MFT is assumed to meet these noise requirements with the use of the nozzle incorporated into the engine design. The nozzle is an axisymmetric concept with a plug. Because there is an assumption being made that the nozzle will be able to achieve twelve to seventeen decibels in noise reduction, the engine is down-scaled in thrust to 75% of its original thrust. This reduction further helps to reduce noise. It has been shown that this scaling ratio will drop the exit velocity by 375 feet per second, which results in additional suppression of 3-4 decibels.

## 8.0 Structures

### 8.1 Material Selection

The average temperature of the aircraft at cruise is 400 degrees Fahrenheit. The hottest regions of the aircraft will be the nose cone and the leading edges of the wing and canard. At those areas the temperature will be at a maximum of 450 degrees Fahrenheit. Figure 8.1.1 shows some of the temperatures at certain locations on the aircraft.

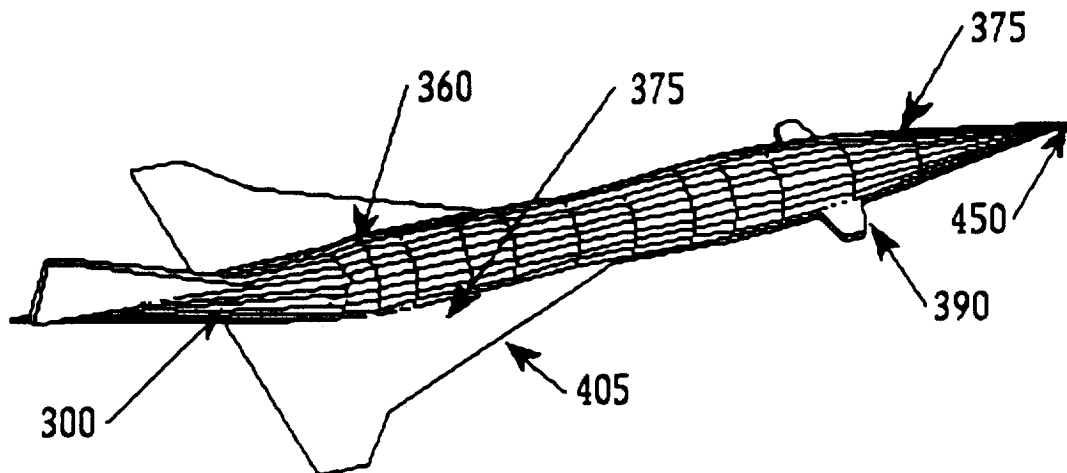


**Figure 8.1.1: Aircraft Temperatures (°F)**

Constructing an aircraft entirely of aluminum such as aluminum 7075 would keep the cost of the aircraft low. Because the typical temperature limitation of aluminum is 250-300 degrees Fahrenheit, aluminum standard on subsonic aircraft construction can not be used for the entire aircraft. Titanium could be used for the entire aircraft since it has a temperature limit that is well above 450

degrees Fahrenheit. The problem with titanium is that manufacturing costs would be excessive. Certainly, the areas that will exceed 400 degrees will be utilizing titanium since they are critical areas. Thus, a compromise between the use of an aluminum alloy, aluminum-lithium, and titanium is utilized on the aircraft. Aluminum-lithium is used over conventional aluminum because of its increased stiffness, fatigue performance, temperature resistance, and lighter weight. Figure 8.1.2 shows the types of materials that the skin and high lift devices will be made of.

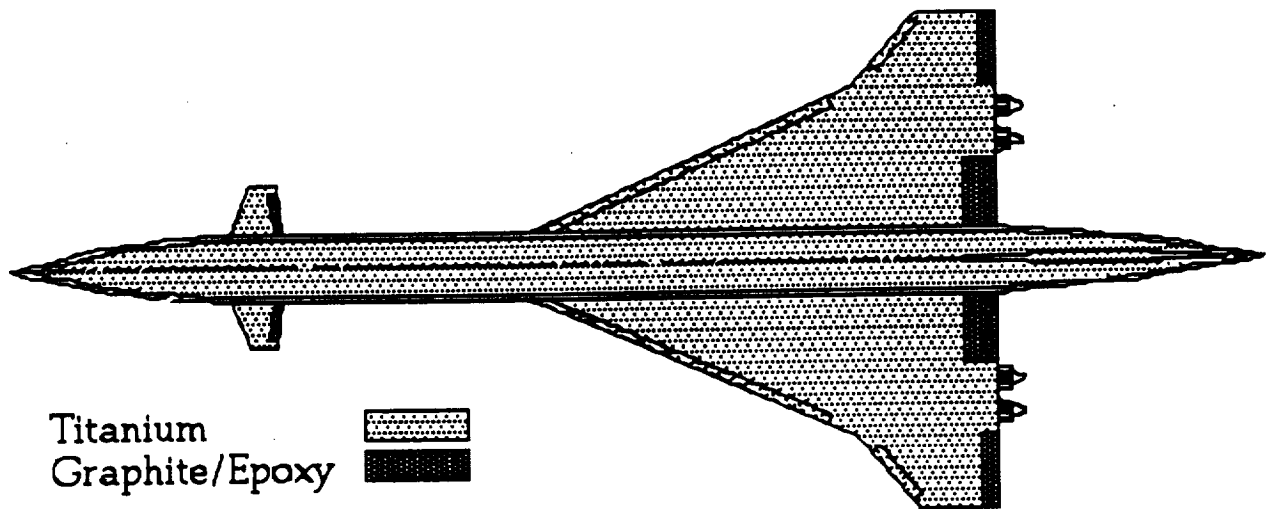


**Figure 8.1.2: Exterior Materials**

The materials that will be used on the interior of the aircraft, which consists of the frames, ribs, spars, and stringers, are shown in Figure 8.1.3



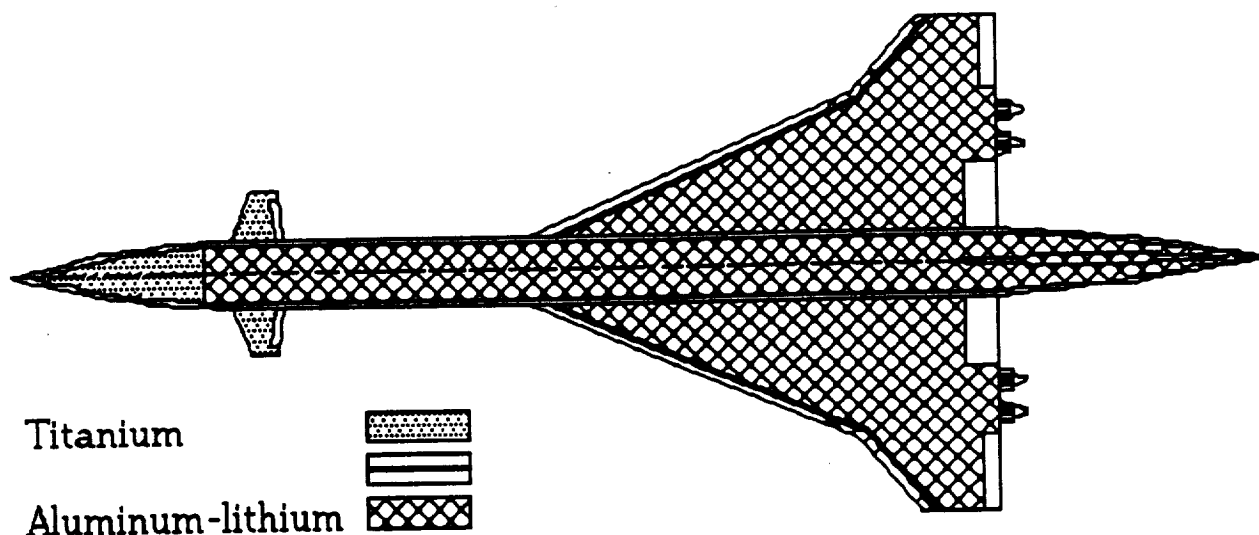
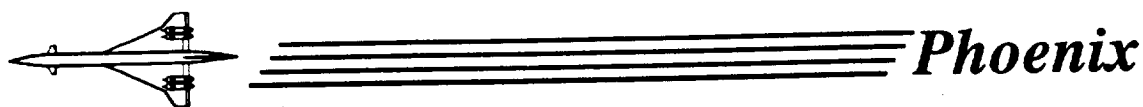


Figure 8.1.3: Interior Materials

## 8.2 Wing Structure

The structural layout of Phoenix's double delta wing is shown in Figure 8.2.1.

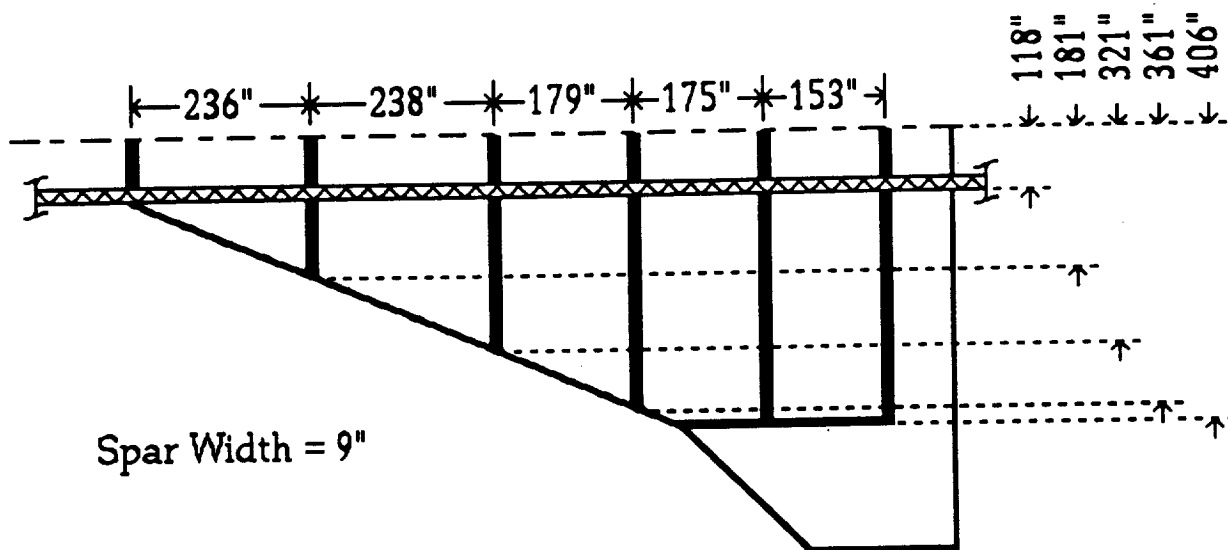
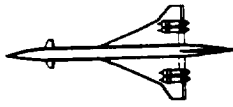


Figure 8.2.1: Wing Structural Layout



# *Phoenix*

The wing is designed using six aluminum-lithium spars. These spars create five distinct wing boxes which simplify the manufacturing of the aircraft and enhance structural integrity. These boxes are predominately fuel cells. Leading edge components and the skin consist of titanium due to the high temperatures experienced in these areas during supersonic flight. The remainder of the wing is constructed of aluminum-lithium. Not shown in the above figure are the ribs. The ribs are stiffened flat panels with cutouts where permissible to save weight.

### 8.3 Fuselage

The design of the fuselage is a conventional semi-monocoque structure. Most of the fuselage structure will utilize aluminum-lithium. This includes the frames, bulkheads, and stringers. The outside skin of the fuselage will consist of titanium. Figure 8.3.1 shows the geometry of the frames and stringers. Figure 8.3.2 shows the placement of the frames and stringers over the entire aircraft.

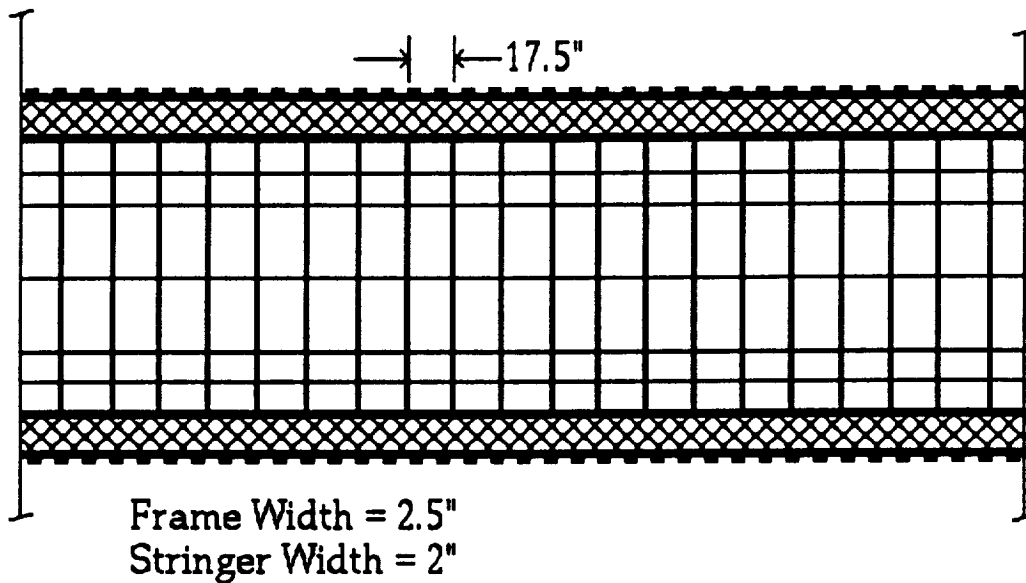
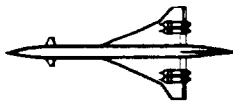


Figure 8.3.1: Frame/Stringer Geometry

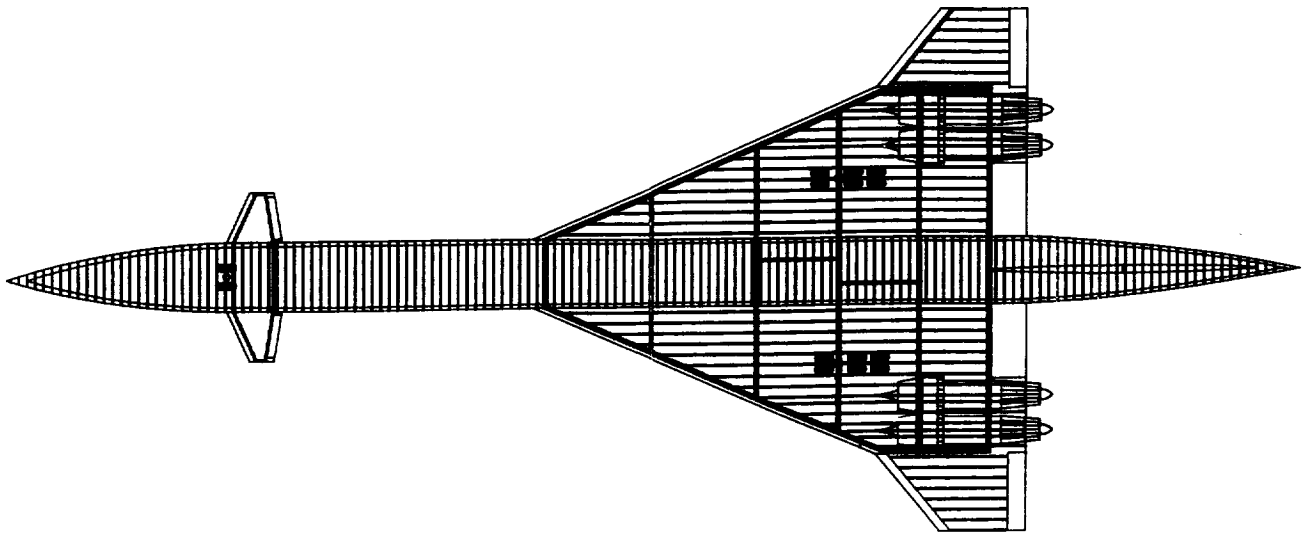
The fuselage design itself is of a fail-safe concept. Thus, the structure will support designated loads if one member fails, or if extensive damage occurs to the structure. The nose cone structural components will utilize titanium because of the highest temperatures at this area.

#### 8.4 Canards

The canard frames and skin are constructed of titanium because of the high temperatures in this region. Graphite-epoxy composites are used for the control surfaces to help manage weight. Figure 8.4.1 shows the canard structure.

# PHOENIX

Figure 8.3.2 - Frames and Stringers



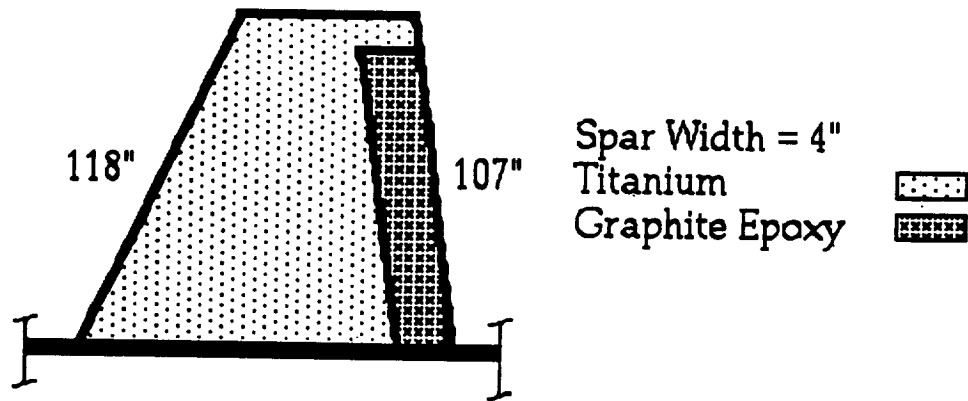


**Figure 8.4.1: Canard Structure**

### 8.5 Vertical Tail

All of the vertical tail structure is composed of aluminum-lithium, except for the skin which is titanium.

### 8.6 V-n Diagram

The V-n diagram was calculated and compared to the gust scenarios of sea-level to 20,000 feet and 60,000 feet. Two case of gust envelopes have been calculated to see critical design areas. For the sea-level to 20,000 feet criteria, shown in figure 8.6.1, it is shown that the aircraft is gust sensitive and must be designed for this scenario. For the 60,000 feet gust envelope evaluation, shown in figure 8.6.2, gust loading is not critical and falls well within the maneuvering diagram.

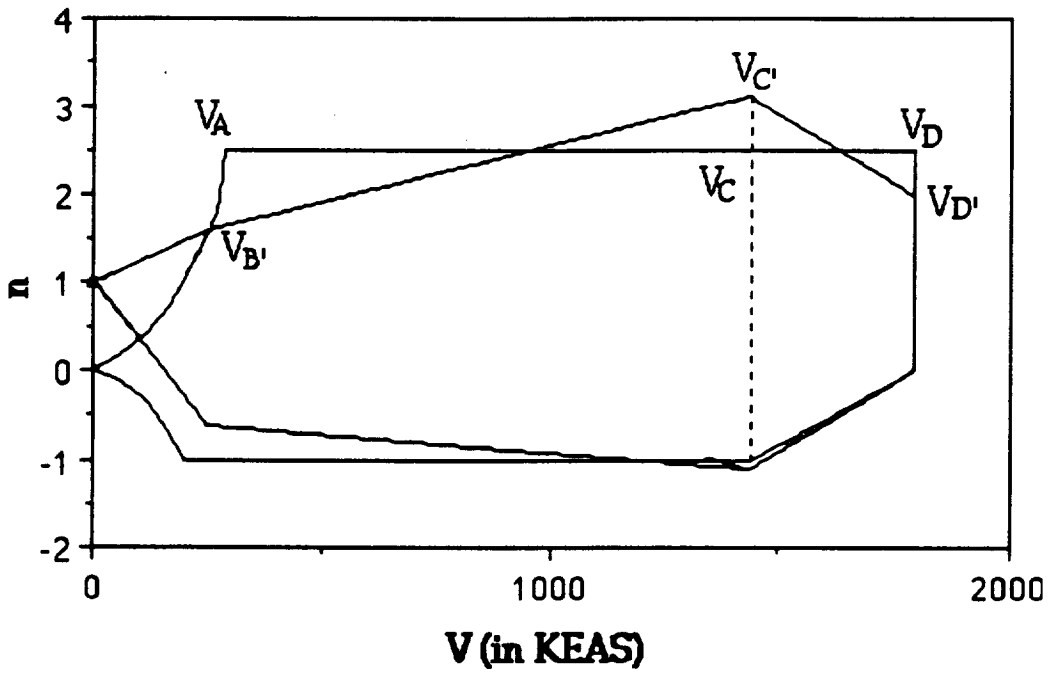
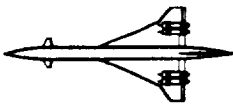


Figure 8.6.1: V-n Diagram for gust at Sea-level to 20,000 feet

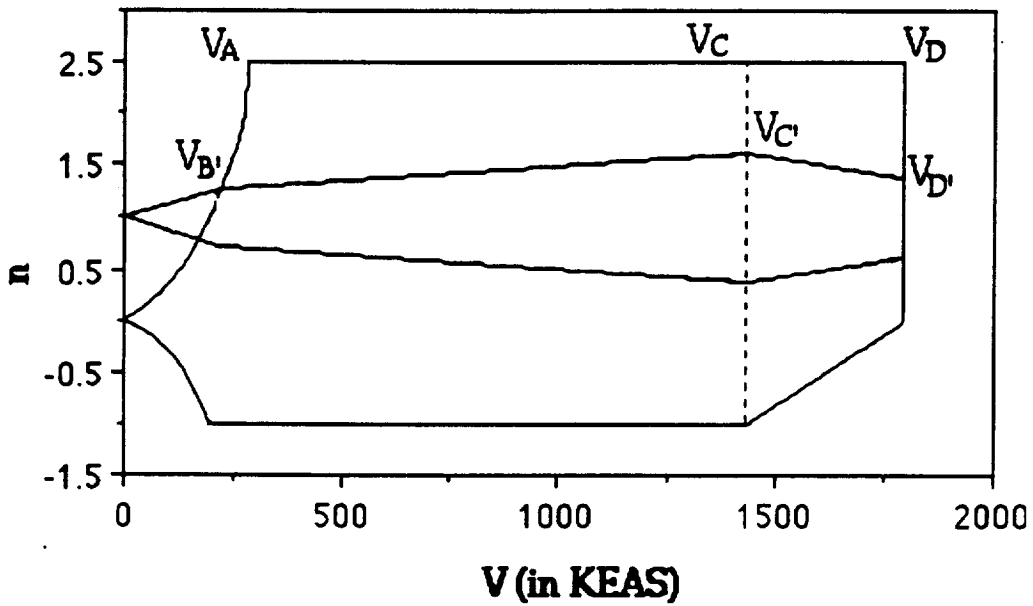
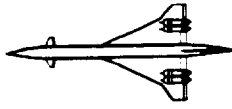


Figure 8.6.2: V-n Diagram for gust at 60,000 feet



## **9.0 Systems Integration**

Primary systems incorporated into the Phoenix design are air-conditioning, anti-icing, electrical, hydraulic, fuel, water systems, avionics, and flight control. This is shown in Figure 9.0.1.

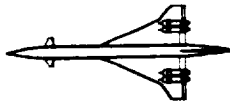
### **9.1 Air-conditioning System**

Two large air-conditioning packs are located in the belly of the fuselage. This placement facilitates service truck hook-up for ground servicing. The air-conditioning units are electrically connected to the auxiliary power unit (APU). The APU can provide power for ground operation of the air conditioning units as well as cold engine start.

Cooled air is piped from the air-conditioning units during flight and directed to the cargo compartment, avionics, radar, and along leading edges of both canard and wing to reduce stagnation temperatures at these points. Conditioned air is directed into the fuselage cabin at three main locations, each at a class divider. One is centrally directed into first class. The other two, one for each business section, are also centrally directed into each section.

### **9.2 Anti-Icing System**

During certain stages of ground operation and in flight, high pressure air is bled from the engines to heat the leading edges of the canard and wings. The heating provided will prevent a build-up of ice on these surfaces.



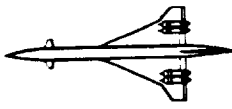
through the fuselage at this location. The remaining tanks are integral fuel tanks divided equally between the two wings. Placing fuel in the wings enhances the aeroelastic damping of the structure. All fuel tanks are located away from critical areas, including engine locations and landing gear stowage. If damage should occur in any of these areas, damage to fuel tanks will be minimized.

Each fuel tank has its own pumping and baffle system. To enhance engine performance, fuel lines are directed along the leading edge of the wing to increase the fuel's enthalpy prior to entering the engine. All fuel tanks are centered around the aircraft's center of gravity. The entire fuel system is managed by the fuel management system, a subsystem of the flight control system. The objective of fuel management will be to maintain the CG close to the MAC. Minimum trim drag is realized for this case. During flight, the fuel management system is capable of maintaining the CG within 0.6% MAC of its takeoff location.

## 9.6 Water System

Several water tanks holding a total of 1000 pounds of water provides the needed water to all galleys and lavatories. The required piping to provide water convenience is incorporated into the design. A third of this capacity is electrically heated to provide hot water. Gray water is collected in a disposal tank and emptied during ground servicing.





### 9.3 Electrical System

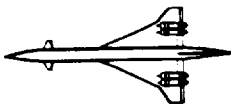
Electrical power is critical to Phoenix. The flight control system requires an uninterrupted supply of electrical energy, as do the electro-hydrostatic (EHS) actuators. System redundancy is high for this critical system. Two independent electrical systems are used in the design. Each system is powered by a separate pair of engines. Additional redundant generating capabilities exist in the auxiliary power unit (APU) and the Ram Air Turbine (RAT). Neither of these devices operates during normal flight conditions. The RAT is automatically deployed when the power level of the electrical system degenerates to a predetermined level. One additional level of redundancy exists in the battery system. The batteries will only supply flight critical systems and are designed to provide a continuous duty cycle.

### 9.4 Hydraulic System

A hydraulic system is required to operate the brakes and to cycle the landing gear. Phoenix uses two separate hydraulic systems. Each system operates independently and has the capability to satisfy all hydraulic requirements.

### 9.5 Fuel System

Phoenix incorporates seven distinct fuel tanks. A single bladder tank is located in the fuselage forward of the main landing gear stowage area. This tank is structurally protected by the wing box which passes



## 9.7 Avionics Systems

The avionics suite envisioned for Phoenix will perform these flight-critical functions: communications; navigation; data processing and display. Additionally, Phoenix affords passengers unique possibilities for entertainment as well as support for data processing and transmission. These additional functions will be managed by dedicated sections of the avionics package aboard Phoenix. Development of the suite will be driven by considerations of life cycle costs, technology level and maintainability.

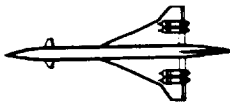
A conceptual representation of the flight deck layout has not been presented although a glass flight deck is envisioned for Phoenix. Current advances in flight deck design are occurring at a tremendous rate. An attempt to model a layout of Phoenix's flight deck would likely not be representative of the final layout. Adequate space has been allocated to the flight deck for the needed systems.

### 9.7.1 Communications

Phoenix will incorporate standard communication devices within the avionics suite. These devices will allow data and voice transmission over both UHF and VHF bands. Additionally, the capability of secure data transmission will be offered as a service to both airline and passenger.

### 9.7.2 Navigation

Phoenix will be equipped with an inertial navigation system (INS).



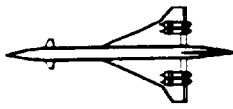
The system will incorporate sensors and processing capability necessary to accurately and safely navigate Phoenix around the globe. The cost of an INS system is not expected to severely impact the overall cost of the avionics system. Compatibility with existing tactical aircraft (TACAN) and global positional system (GPS) navigation systems is being considered for Phoenix.

### 9.7.3 Data Processing and Display

In addition to performing flight control, the Phoenix computers (Section 9.7) will share the function of processing sensor data input for display to the flight crew. To facilitate data display, Phoenix utilizes a glass flight deck design. Immense computational capability will be required for Phoenix. In addition to providing flight control and air-data processing, the on-board computers will need to generate the involved graphic interface of the synthetic vision system.

### 9.8 Flight Control System

Due to poor lateral performance characteristics, Phoenix will be equipped with a digital Flight Control System (FCS). The core of the FCS will be three redundant flight control computers powered by the main electrical system with battery backup. Any one computer can operate Phoenix individually. In addition to flight control, the FCS will perform in-flight CG management functions. The remainder of the flight control system is comprised of fiber-optic connections from the FCS to control surface actuators and fuel pumps. The actuators used aboard Phoenix



# Phoenix

are EHS. These devices incorporate a small electrically-commanded actuator with an integral hydraulic pump and reservoir. Two primary advantages are achieved when using an EHS system compared to a conventional hydraulic system: less system complexity and weight; built-in redundancy when multiple actuators are used. EHS actuators represent untried technology for an aircraft like Phoenix. Heat transfer is an issue in the structural locations where EHS actuators are used. This concern will need to be addressed in the design of the final flight control system.

Another critical function of the flight control system is CG management. The computers onboard Phoenix will command and monitor the transfer of fuel throughout various fuel tanks so that the CG is located optimally both in flight and on the ground.

## **10.0 Landing Gear**

### **10.1 Configuration**

The design and placement of landing gear in a HCST is a challenging problem. The combination of high dynamic loading and small storage volume combine to create a challenging engineering problem.

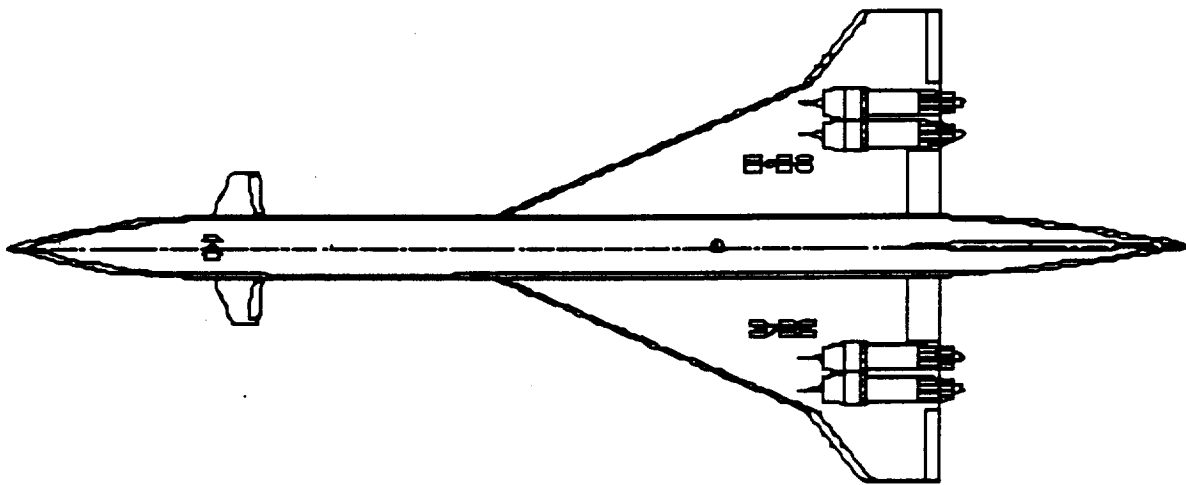


**Figure 10.1.1: Landing Gear Layout**

A standard tricycle configuration was used for the landing gear. This is shown in Figure 10.1.1. A weight of 500,000 lbs. was used in determining how many and what type of tires needed to use for the landing gear. This allowed for possible growth of the aircraft during the design period. The tires used are 40" in diameter and have a width of 15.5". Table 10.1.1 shows additional tire data.

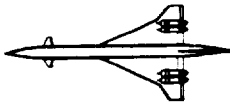


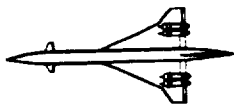
Table 10.1.1: Landing Gear Tire Data (per tire)

Tire Pressure	180 psi
Maximum Speed	235 mph
Loaded Radius	16.1 inches
Flat Tire Radius	11.6 inches
Minimum Diameter	39.1 inches
Footprint Area	326 square inches
Maximum Loading (per wheel)	58,600 pounds

The front landing gear has two wheels and the main landing gear has two bogeys with six wheels each. Three or four bogeys were originally considered for the main landing gear, but not having the option of retracting the gear into the wings limited the design to two bogeys. Having six-wheel bogeys in the rear, the plane would want track in a straight line, making it difficult to steer. For this reason, the rear gear is steerable. The length of the bogey is 169 inches and the width is 41 inches. The diameter of the struts for the main landing gear is 19 inches. The diameter of the strut for the front landing gear is 9 inches.

The actuators in the rear would retract or extend, steering the bogeys. The right and left bogeys are linked together through a steering control system; a "steer-by-wire" system.

The front landing gear is located 42.8 feet from the nose of the aircraft and the main landing gear is located 162.0 feet from the nose. The center of gravity of the plane at take-off is located at 149.7 feet



from the nose of the plane. This means that the nose gear is carrying 14% of the load and the main gear is carrying 91% of the load. These values are well within the loading capabilities of the gear.

Due to the thin wing, it was necessary to stow the landing gear entirely in the fuselage. It was also necessary to have the tires remain in a vertical attitude as they retracted. By doing this the height of the landing gear in the stowed position is minimized. This retraction scheme is shown in Figure 10.1.2.

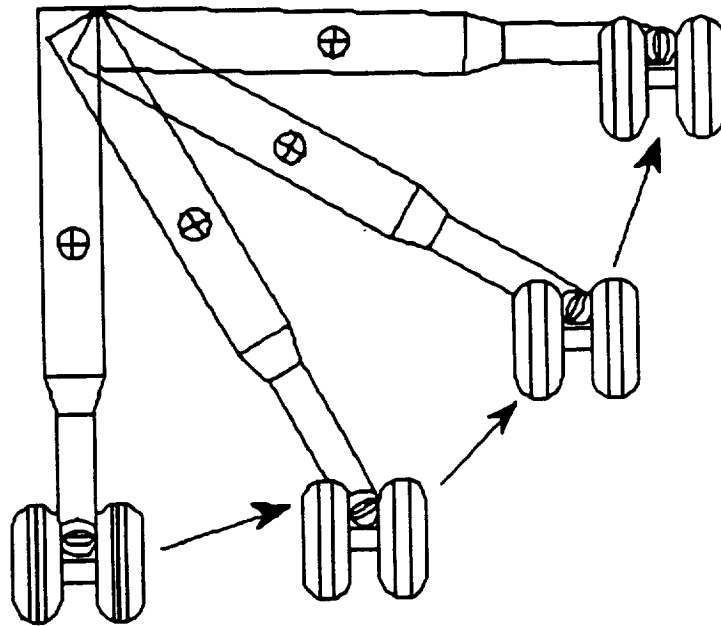
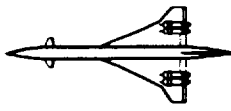


**Figure 10.1.2: Main Landing Gear Retraction Scheme**

The height of the gear in the stowed position was smallest when it is retracted in this manner. The height of the tires is less than the width of the tires, the axle, and the length of the bogey. It is also necessary to retract the gear diagonally into the fuselage because the bogeys rest one in front of the other in the retracted position. The



retraction paths are shown in Figure 10.1.3.

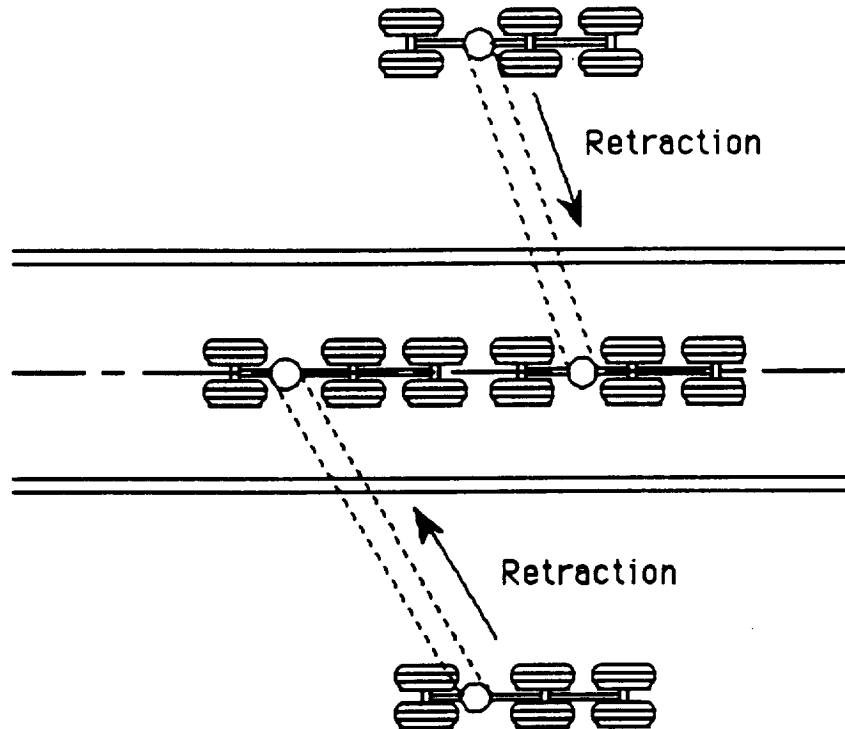


**Figure 10.1.3: Main Landing Gear Retraction Path**

Figure 10.1.3 shows the gear in both the retracted and extended positions. The angles that the gear retracts through are different because it was necessary that the main oleos be at the same location along the fuselage so that they could be mounted on the same strut. The landing gear can also be extended and retracted by mechanical means in an emergency situation.

## 10.2 Compliance

This placement of the gear allows it to meet both the turn-over and tip-over criteria. Figure 10.2.1 shows that the combination of the main gear placement and the upsweep on the tail cone allows for a



takeoff rotation of at least  $15^\circ$ . Figure 10.2.1 also shows the tip-over angle of  $34^\circ$ . If the tip-over angle was less than the rotation angle, the aircraft would over-rotate on takeoff.

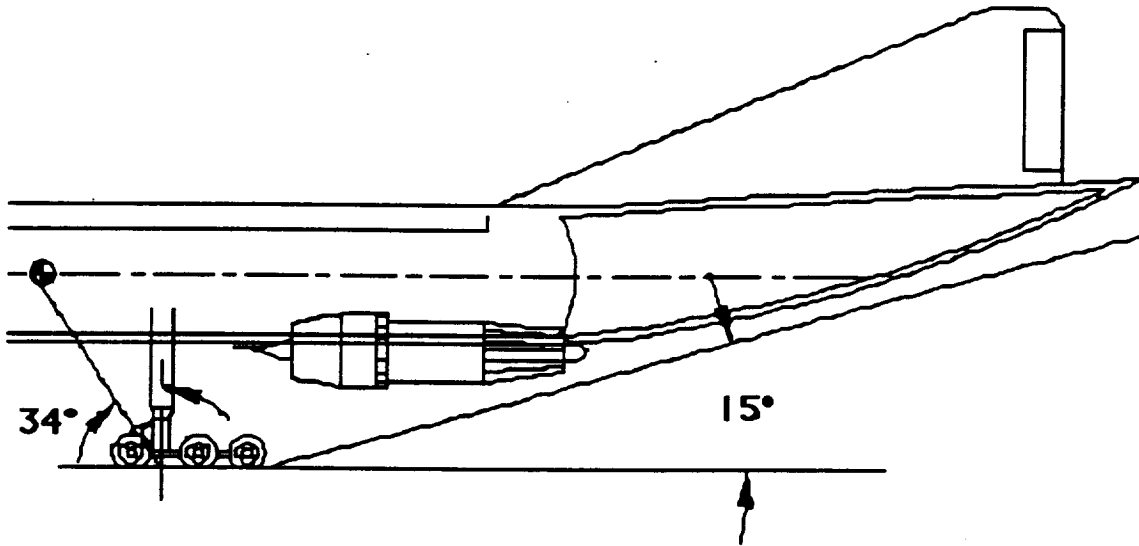


**Figure 10.2.1: Tip-over and Takeoff Rotation**

It is necessary that the turn-over angle for the aircraft be greater than  $63^\circ$  so that it does not turn over on its side when making tight turns on the ground. The turn-over angle for this configuration is  $43.1^\circ$ , so Phoenix will be stable and not turn over when maneuvering on the ground. This is shown in Figure 10.2.2.

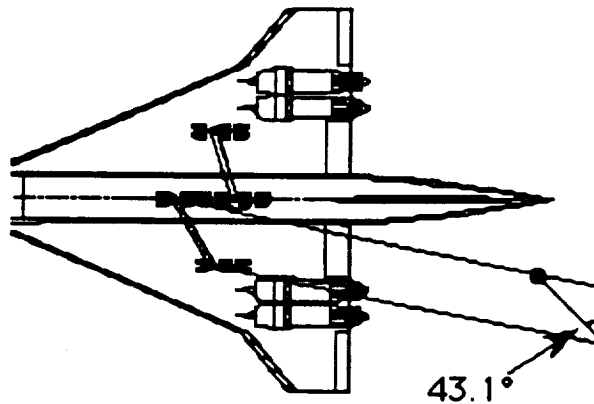
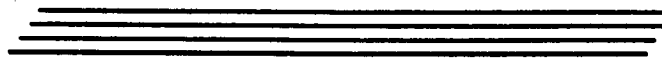
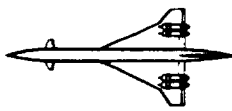
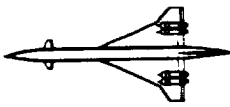


**Figure 10.2.2: Turn-Over Criteria**

The Load Classification Number (LCN) for this gear configuration is 92. This number is based on an Equivalent Single Wheel Loading (ESWL) of 69,000 pounds. The ESWL was computed by using a method similar to that found in Roskam. The load of one of the main oleos was divided by 3.2 because of the six wheels on each bogey. (Reference 11 used a divisor of 1.33 for a two wheel bogey)



## **11.0 Stability and Control**

### **11.1 Weight and Balance**

The weight estimations of aircraft components were calculated from statistical equations shown in Reference 5 and 12. A summary of Phoenix's various weights is shown in Table 11.1.1. The weight breakdown with their relative location is provided in Table 11.1.2. Composites were assumed to be incorporated with a 10% overall weight savings for all structural components, excluding landing gear. Additionally, a 5% weight savings was assumed for non-electrical fixed equipment. The resulting takeoff weight is 455000 pounds.

**Table 11.1.1: Aircraft Weight Breakdown**

<b>Summary</b>	<b>Weight (lbs.)</b>
Weight (Takeoff)	455,000
Weight (Empty)	198,000
Weight - Structure	88,250
Weight - Power Plant	67,330
Weight - Fixed Equipment	38,180
Weight - Payload	31,500
Weight - Crew	1,400
Weight - Fuel	221,840
Weight - Trapped Fuel and Oil	2,280

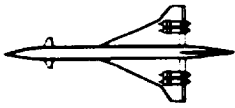
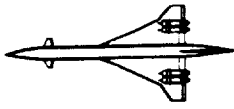


**Table 11.1.2: Aircraft Weight Component Breakdown and Location**

	Weight (lbs.)	x-Location (inches)	z-Location (inches)
<b>Structure</b>			
Wing	39,120	1993	-36
Canard	1,950	644	-30
Vertical Tail	3,010	2805	144
Fuselage	28,510	1494	0
Nacelle	4890	2316	-108
Main Landing Gear	9,400	2015	-40
Nose Landing Gear	1,390	584	-25
<b>Power Plant</b>			
Engines	30,990	2316	-108
Fuel System	1700	1993	-36
Propulsion System	5270	2316	-108
<b>Fixed Equipment</b>			
Flight Control System	4,620	1490	0
Hydraulic and Pneumatic System	3,720	2316	0
Electrical System	2,700	1494	0
Instrumentation, Avionics, and Electronics	2,960	762	0
Air-conditioning, Pressurization, Anti- and De-icing	4030	1173	-36
Oxygen System	240	1495	0
Auxiliary Power Unit	370	2630	-36
Furnishings	15,310	1494	0
Baggage and Cargo Handling	720	887	0
Operational Items	2,000	1681	0
Paint	1,380	1494	0



### 11.2 Moments of Inertia

The moments of inertia are calculated from the weight breakdown shown in Table 11.2.1. These values were determined by assuming individual moments of inertia of small components are negligible; these components are treated as point masses.

**Table 11.2.1: Moments of Inertia**

Ixx	2.14 E+7
Iyy	3.26 E+6
Izz	1.62 E+5
Ixy	8.79 E+3
Iyz	9.31 E+3
Ixz	-5.69 E+5

### 11.3 Excursion Plot

Figure 11.3.1 shows the resulting center of gravity excursion while the aircraft is at different stages of loading or flight. During flight, the total excursion is 4 inches, 0.6% of MAC.

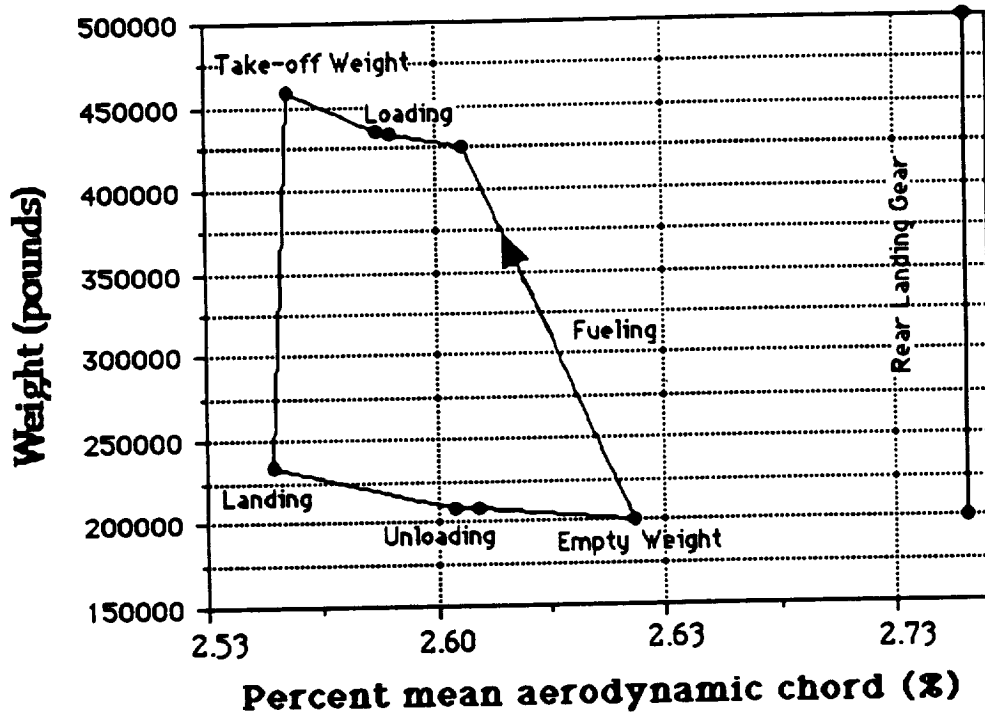
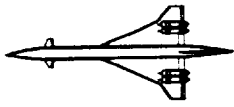
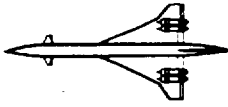


Figure 11.3.1: Excursion Plot

#### 11.4 Static Stability

As determined from initial sizing by methods given by Reference 13, this aircraft is inherently, statically stable for the longitudinal and lateral axes. The empennage sizing calculated is the basis for the stability derivatives presented in Tables 11.4.1 and 11.4.2. Presented are derivatives for take-off, subsonic cruise, and supersonic cruise conditions. Calculations for each stability derivative are based upon various geometric and aerodynamic relationships described in Reference 13.

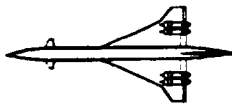
These derivatives are used as input to determine static and dynamic stability and control behavior of Phoenix. The relative magnitudes of each derivative relates the sensitivity of the aircraft's



response to air forces. The closer the magnitude is to zero, the less sensitive the aircraft is to external disturbances (assuming small perturbations). As seen in Table 11.4.1, Phoenix is most sensitive to pitch rate for all conditions.

**Table 11.4.1: Longitudinal-Directional Stability Derivatives**

Longitudinal	Sub. cruise	Sup. cruise	T/O
$C_{m_u}$ :	-0.03	-0.01	-0.09
$C_{m_{\alpha f}}$ :	-0.09	-0.33	-0.09
$C_{m_{\alpha f}(\dot{\alpha})}$ :	-0.12	-0.12	0.00
$C_{m_q}$ :	-3.83	-18.98	-3.51
$C_{m_{T_u}}$ :	0.00	0.00	-0.02
$C_{m_{T(\alpha f)}}$ :	0.00	0.00	0.00
$C_{l_u}$ :	0.04	0.01	0.01
$C_{l_{\alpha f}}$ :	1.48	4.91	1.48
$C_{l_{\alpha f}(\dot{\alpha})}$ :	0.10	0.05	0.00
$C_{l_q}$ :	2.67	4.35	2.64
$C_{d_{\alpha f}}$ :	0.14	0.14	0.14
$C_{d_u}$ :	0.00	0.00	0.00
$C_{t_{x_u}}$ :	-0.06	0.00	-0.36
$C_{l_{dc}}$ :	0.01	0.01	0.01
$C_{d_{dc}}$ :	0.00	0.00	0.01
$C_{m_{dc}}$ :	-0.01	-0.01	-0.01

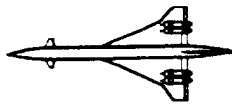


This sensitivity is most obvious during supersonic cruise. This is expected since the faster an aircraft travels, the more violent are the reaction to sudden changes. The overall low magnitudes of stability derivatives demonstrate Phoenix to be controllable in all regimes of flight. Any derivatives deemed high can be easily compensated if desired.

**Table 11.4.2: Lateral Directional Stability Derivatives**

Lateral-Directional	Sub. cruise	Sup. cruise	T/O
$Cl_{b\dot{\alpha}}$ :	-0.05	0.00	-0.28
$Cl_p$ :	-0.33	-0.13	-0.24
$Cl_r$ :	0.22	No method	0.70
$Cl_{\dot{\alpha}}$ :	0.04	0.01	0.00
$Cl_{\dot{r}}$ :	0.00	0.00	0.00
$Cn_{b\dot{\alpha}}$ :	0.05	0.00	0.05
$Cn_p$ :	0.08	-0.03	-0.45
$Cn_r$ :	-0.09	No method	-0.17
$Cn_{\dot{\alpha}}$ :	-0.01	0.00	0.00
$Cn_{\dot{r}}$ :	-0.01	0.00	-0.01
$Cy_{b\dot{\alpha}}$ :	-0.15	0.00	-0.15
$Cy_p$ :	-0.03	0.00	0.00
$Cy_r$ :	0.11	No method	0.11
$Cy_{\dot{\alpha}}$ :	0.00	0.00	0.00
$Cy_{\dot{r}}$ :	0.01	0.00	0.01





Regarding lateral static stability, the control power derivative is found to be acceptable for the rudder size initially determined from class I sizing methods. This allowance meets the minimum controllability requirement for a one engine inoperative scenario.

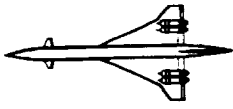
### 11.5 Dynamic Stability

Concerning dynamic longitudinal stability, the undamped natural frequency and damping ratios for the phugoid and short-period modes are listed in Table 11.5.1. These values were computed using stability derivatives under steady state flight conditions.

**Table 11.5.1: Literal Factors for Varying Flight Conditions**

	Sub. cruise	Sup. cruise	T/O
Phugoid natural frequency (rad/sec)	0.054	0.019	0.163
Phugoid damping ratio	0.255	0.074	0.426
Short-period natural frequency (rad/sec)	2.01	4.63	1.29
Short-period damping ratio	1.20	0.64	1.53

An important aspect of the literal factors is to determine a safe

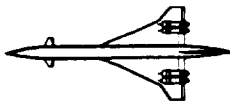


operating frequency range for the aircraft. From a structural standpoint, the natural frequency of the material for the aircraft must coincide with neither the phugoid nor short period frequencies. A match in frequencies will excite the material and result in catastrophic failure. The literal factors for Phoenix are not a problem in this sense and does not constrain materials used in building the aircraft.

The damping ratios smooth aircraft motion by reducing the sinusoidal tendencies of flight. Phoenix is sufficiently damped to provide optimum comfort for passengers and good flying qualities for the pilots.

The flight categories investigated for handling quality evaluation were for subsonic and supersonic cruise conditions (Category B) and take-off (Category C). The subsonic portion of Category B is for a Mach 0.85 at 30,000 feet. and the supersonic portion for Mach 2.5 at 60,000 feet. The Category C condition is for Mach 0.25 at sea level. The MIL-F-8785C (Reference 14) is used for the evaluation of flight handling qualities due to its consideration as a standard for both military and civil aircraft. By this standard, the phugoid damping ratio is found to fall within level 1 handling quality for Category B and Category C flight. The short-period frequency requirement for Category B established a level 1 rating while the Category C short-period frequency classed borderline level 1 and 2. The short-period damping ratio for both Category B and Category C phases demonstrated level 1 ratings.

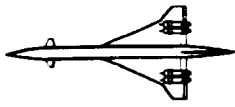
Dynamic lateral-directional stability analysis results are presented in Table 11.5.2. Handling qualities for roll evaluation are based upon the



determined aircraft roll time constant. Both Category B and C flight phases ranked level 3 for this criterion. To fulfill the level 1 requirement, a stability augmentation system (SAS) will be incorporated into Phoenix. The desire to achieve level 1 ratings for Category B and C is spurred by safety concerns, especially during supersonic cruise and landing procedures.

Regarding spiral characteristics, the Category C flight phase demonstrates sufficient stability. Using the MIL-F-8785C time-to-double amplitude parameter to evaluate Category B, a handling quality rating for level 3 is achieved. The extent of geometric reconfiguration by means of additional dihedral is considered too great in risk of violating the lateral landing gear clearance criterion to be a feasible solution. The present use of an SAS will provide feedback for the rudder and ailerons to achieve a level 1 spiral handling quality.

Regarding Dutch roll characteristics, the damping ratios for Category B and C flight phases satisfy level 1 requirements in the MIL-F-8785C. The benefit of such damping is increased comfort for passengers. Although rapid rolling and/or bank angle tracking maneuvers are not mission specified for this aircraft, the degree of damping provides additional control for the pilot should a high degree of bank angle become prevalent. Criterion application to the Dutch mode undamped natural frequency yields a level 1 rating for the Category B flight phase, but a subjective rating for Category C. Due to Class III airplanes possibly being excepted from the minimum undamped natural frequency requirement, the rating is not



essentially legitimate and subject to buyer demands.

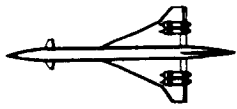
**Table 11.5.2: Dynamic Lateral-Directional Stability Results**

	Sub. cruise	Sup. cruise	T/O
Roll time constant (sec)	5.90	22.69	8.78
Time-to-double amplitude (sec)	0.07	No method	Not needed
Dutch roll undamped, natural frequency rad/sec	7.69	No method	1.56
Dutch roll damping ratio	0.41	No method	0.48

### 11.6 Canard and Empennage Design

Canard and empennage sizing is done in accordance with Reference 13 methods for stability and control determination. The center of gravity location for Phoenix based upon canard area is correlated by means of weight and balance analysis. The aerodynamic center (ac) location for Phoenix is found using geometric and aerodynamic quantities computed by methods given in Reference 13. In allowance for inherent longitudinal static stability, a static margin of 5% is determined as a minimal criterion for a supersonic transport.

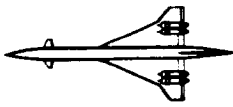
Vertical tail sizing is based upon a 0.0010 per degree value of static directional stability. This value of stability is desired for an inherently



## *Phoenix*

stable aircraft in the lateral sense. A corresponding vertical tail area is found for this provision.

Some extent of SAS compensation is relied upon in sizing consideration. To minimize surface areas for drag reduction, various control surfaces are used in concert with each other to complement the functioning of the canards and empennage surfaces. The use of an SAS may bring to question how standard is the use of such augmentation in aircraft. However, the point that "inherent" or "de-facto" stability of an aircraft is by choice of the designer and not the regulations should be emphasized. As a low to moderate performance aircraft, this supersonic transport is ideally suited to be inherently stable. Yet lateral-directional concerns dictate the need for an SAS. Since maneuverability is not a grave issue for this particular design, other issues such as maintainability, reliability, and cost become primary. The need for increased complexity in control systems and sensor use, some added cost, and additional maintenance associated with "de-facto" stable aircraft is well compensated by improved flyability and a smaller incurred drag penalty.



## 12.0 Performance

### 12.1 Takeoff and Landing

Phoenix needs to satisfy FAR 25 requirements for certification. The customer has directed that these requirements be satisfied for a runway length of 11,000 feet or less. To determine the capabilities of Phoenix, the longitudinal aspect of all phases of the HSCT mission were integrated with time. This evaluation indicated that Phoenix requires a minimum thrust-to-weight ratio of 0.33. This minimum is driven by OEI takeoff performance requirements. Figure 12.1.1 represents the takeoff performance for Phoenix: takeoff roll for all engines operating is 7110 feet.

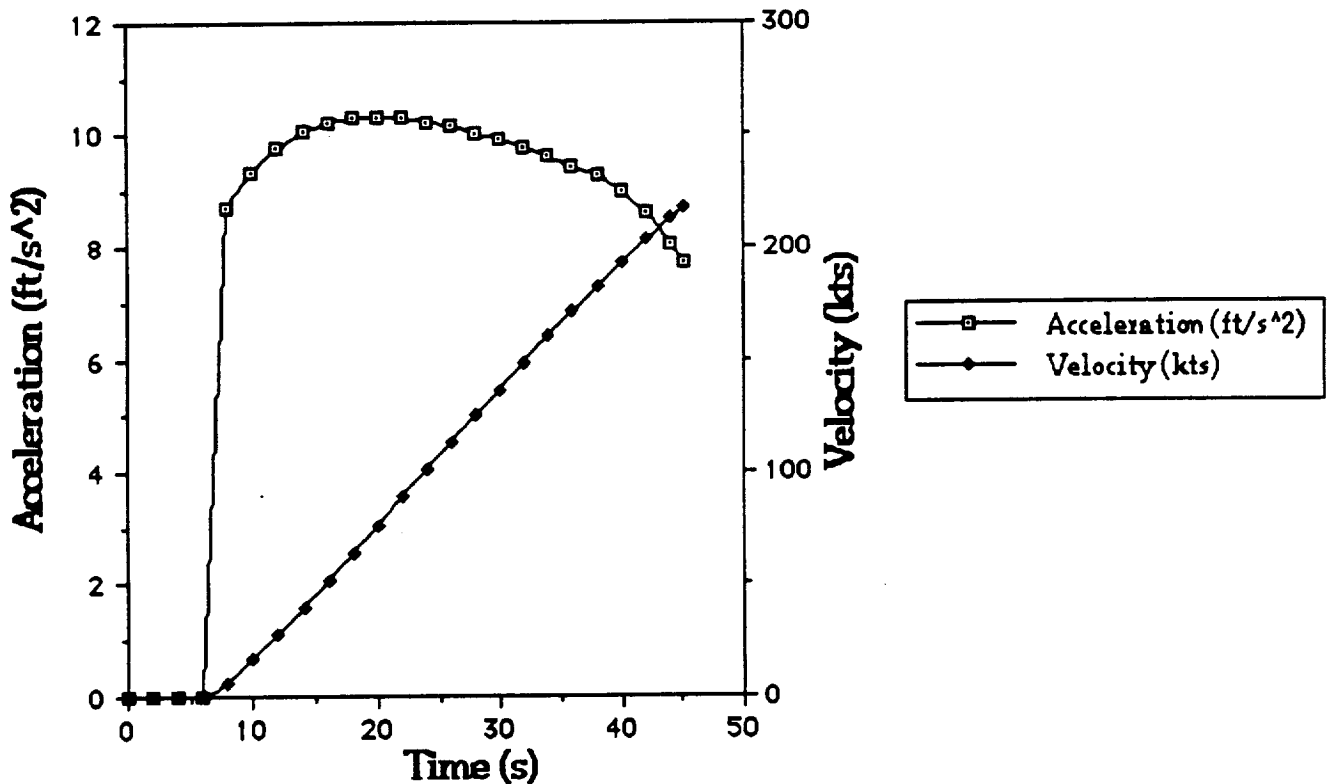
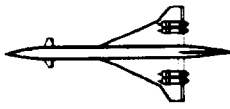


Figure 12.1.1: Takeoff Performance



Maximum horizontal acceleration during the roll is 10.3 feet/sec<sup>2</sup>.

Figure 12.1.2 displays lift and L/D during the roll.

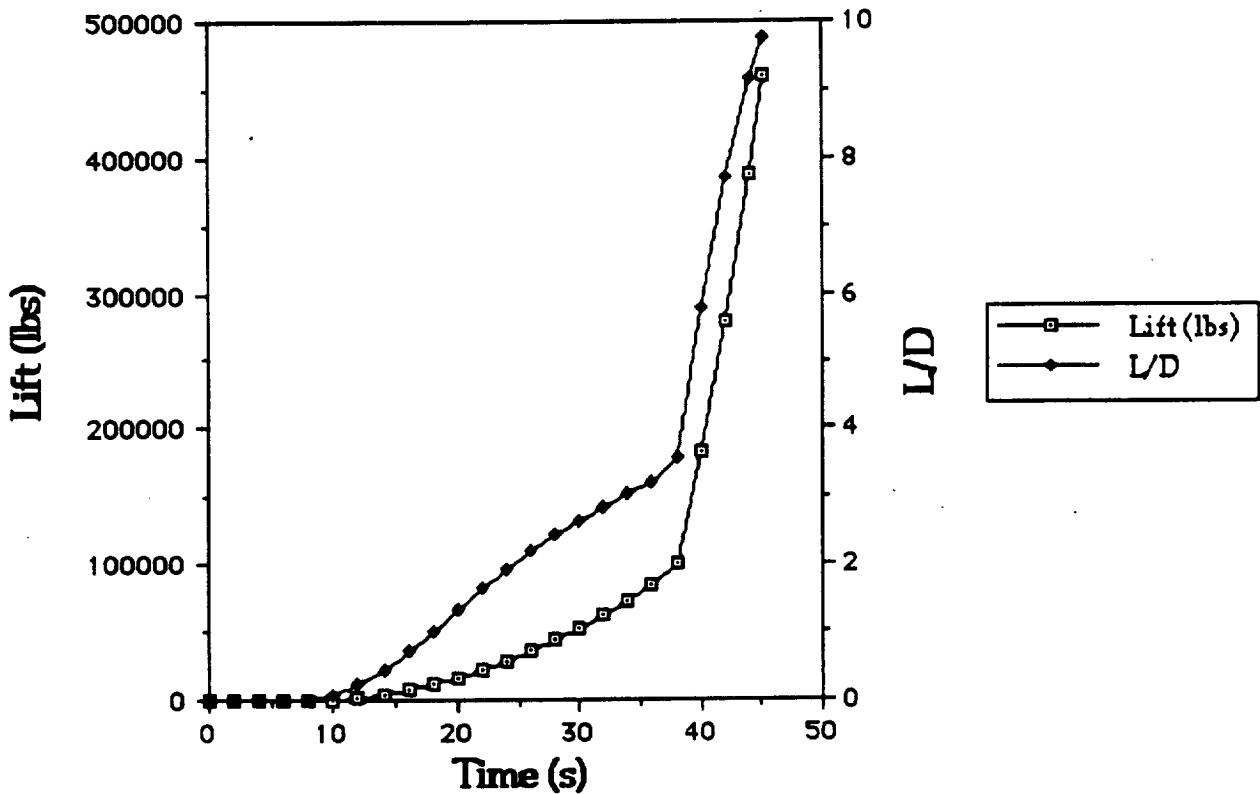


Figure 12.1.2: Lift and L/D During Roll

Decision speed for Phoenix is coincident with rotation speed ( $V_1=V_2$ ). For this reason, any engine failure prior to rotation can be safely contained by rejecting the takeoff roll. Any single engine failure after rotation can be safely managed by continuing the takeoff roll. OEI obstacle clearance for an 11,000 foot runway is 103 feet. This analysis incorporates a pilot delay of 3 seconds at rotation velocity. Critical take-off velocities for Phoenix are:  $V_1 = V_2 = 181$  knots. and  $V_3 = 216$  knots. OEI performance for landing is displayed in Figure 12.1.3.

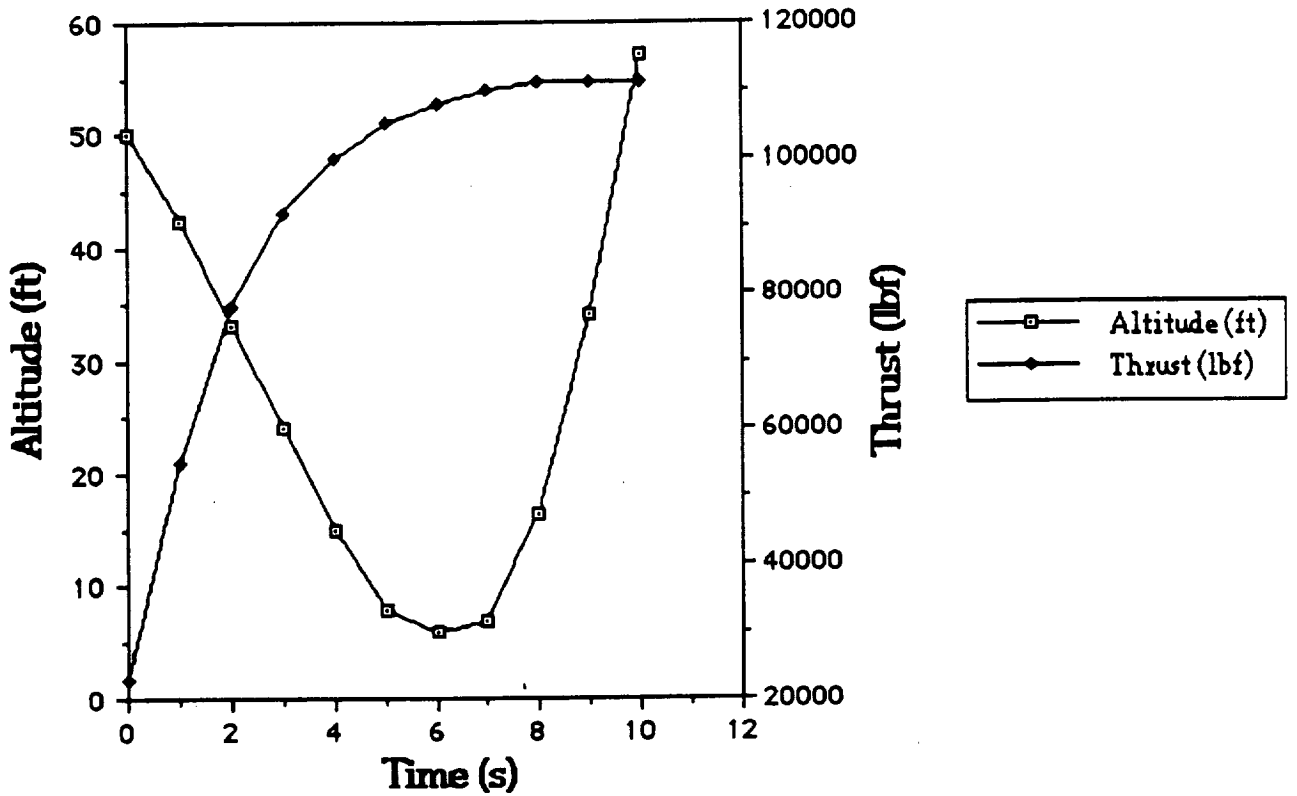
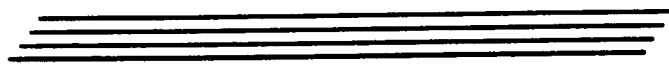
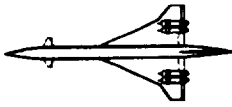
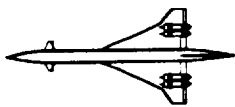


Figure 12.1.3: OEI Performance for Landing

At  $t = 0$  seconds, a go-around is commenced from an altitude of 50 feet AGL with only three of four engines operating at approach setting. Power is applied as Phoenix rejects the approach. The main landing gear's closest approach is 7 feet AGL. Rejected landing weight for this analysis is 80% of gross takeoff weight.

The braking roll for landing is analyzed at 80% gross takeoff weight. Thrust reversers are not utilized. Spoilers are deployed during main landing gear compression to dump lift. Maximum braking roll under dry conditions is 7110 feet following clearance of a 50 feet obstacle at the approach threshold.





## 12.2 Climb

No climb requirements are specified for Phoenix. Standard-day climb performance averages 3150 fpm to an altitude of 30,000 feet for the standard mission profile. While maximum rate of climb for various flight regimes was not calculated, the flight integration program confirmed fully loaded OEI climb rates of 3400 fpm are possible at altitudes below 30,000 feet MSL.

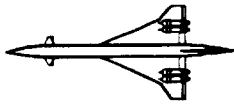
Optimal range is achieved with a flight path angle of 5 degrees for all phases of climb.

## 12.3 Fuel Consumption

At takeoff, Phoenix carries 224,000 lbs of Jet A fuel. Ten percent of this load is required reserves. An additional 9% is expended during climb to cruise altitude. Five percent is expended during descent, approach and landing. The remaining 76% is expended during cruise.

## 12.4 Level Acceleration

Phoenix accelerates from Mach 0.85 to Mach 2.5 at a standard altitude of 30,000 feet. Maximum possible horizontal acceleration at this altitude is 6.53 feet/sec<sup>2</sup>. Passenger comfort dictates a maximum acceleration of 5 feet per sec<sup>2</sup> for 5.5 minutes. This acceleration is maintained by allowing Phoenix to lose altitude (2 degree nose low attitude) while accelerating. Minimum vertical g-load during acceleration is 0.85 g.

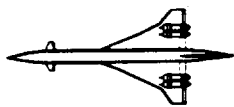


### 12.5 Performance summary

Presented in Table 12.5.1 is a summary for the discussed performance characteristics. All take-off and landing performance for sea level conditions with temperature of 95°F.\* Landing ground roll is evaluated without use of thrust reversers and 80% of the take-off weight.\*\*

**Table 12.5.1: Performance Summary**

T/O Ground Roll*	7150 ft
Landing Ground Roll**	7100 ft
Max. T/O Acceleration	10.3 ft/sec
Max. Sustained Load Factor	2.5 g
Climb Gradient Phase I & II	0.087
Max. Range without Reserves	5150 n.m.



## **13.0 Airport Compatibility**

### **13.1 Noise**

With the engines used on Phoenix , FAR 36, stage 3 can be met with a noise suppression nozzle. With further modifications of a noise reduction system, the more stringent stage 4 requirements will be obtainable with a weight penalty to the aircraft.

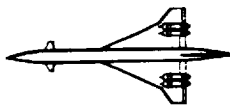
### **13.2 Space Compliance**

The designed length of the aircraft exceeds the current 747-400 length by 38 feet. This will not be a problem since airports will be able to facilitate all maintenance and loading of the aircraft by Phoenix being parked in the diagonal of the 747-400. Door sill height is 16.25 feet which is easily accommodated by current airport terminals.

Weight sizing have shown the takeoff weight of 456,000 pounds being considerably less than the 747-400. This incurs no problems with pavement loading of existing runways.

### **13.3 Maneuverability**

With the design of the steerable landing gear, Phoenix is able to successfully maneuver around existing airport facilities with a turning radius of approximately 120 feet. No additional fillets on runways are required.



## 14.0 Service Requirements and Maintenance

### 14.1 Service Requirements

The ability to maintain and service Phoenix quickly and efficiently is a primary concern. Easy access to components requiring routine maintenance and service is accounted for in the aircraft design. Figure 14.1.1 shows servicing equipment being able to function around the aircraft without interfering with each other.

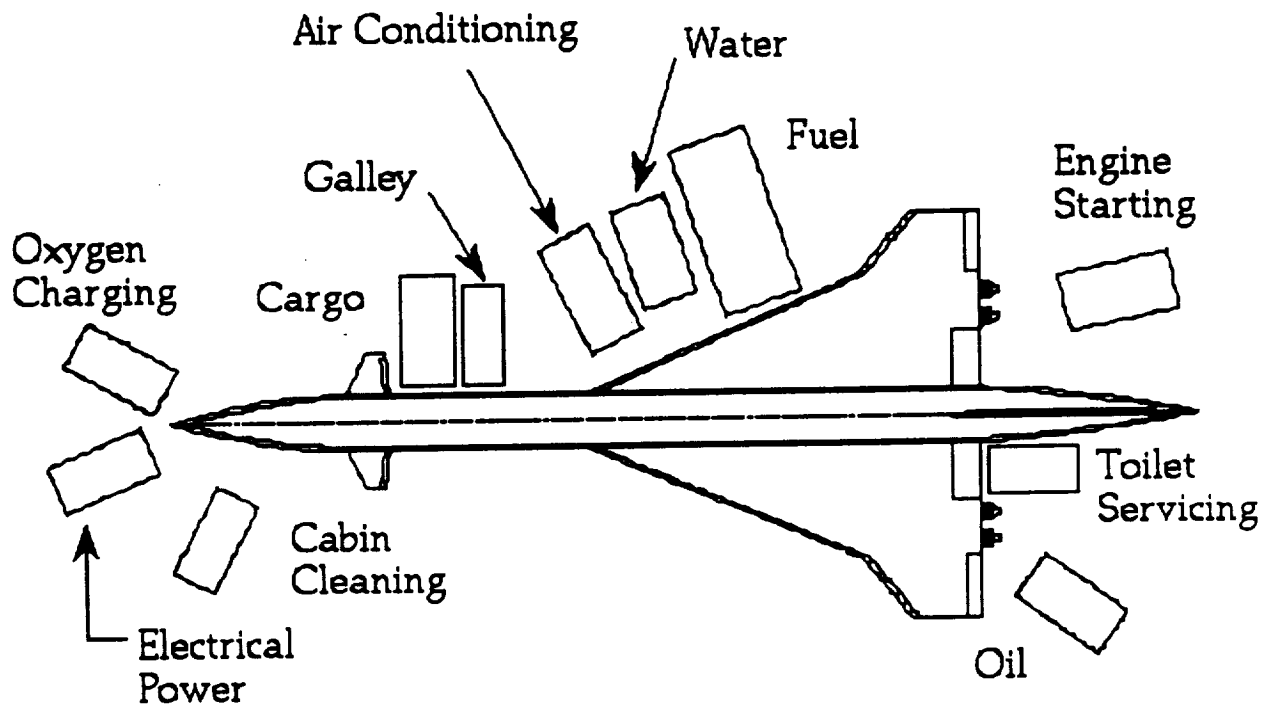
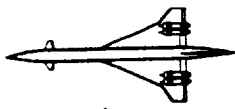


Figure 14.1.1: Aircraft Servicing Diagram

### 14.2 Maintenance

In order to service the wing, there are sufficient inspection panels located on the wing. Larger inspection covers are placed over areas that require frequent attention. These areas include high lift



devices, control systems, and fuel systems. Figure 14.2.1 shows the location of these panels

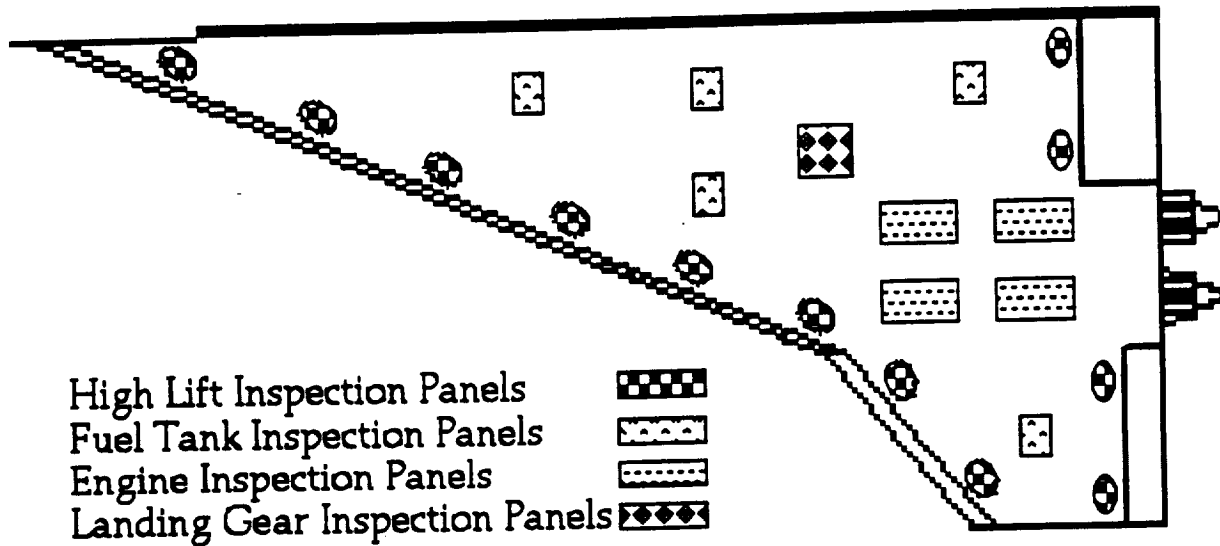


**Figure 14.2.1: Wing Access Panels**

The most significant system on the wing requiring access are the engines. The engines are purposely placed underneath the wings, not only for performance considerations but also for maintenance. The nacelles are removable for easy access to service and remove engines. Figure 14.2.2 shows the breakdown panels of the engines.

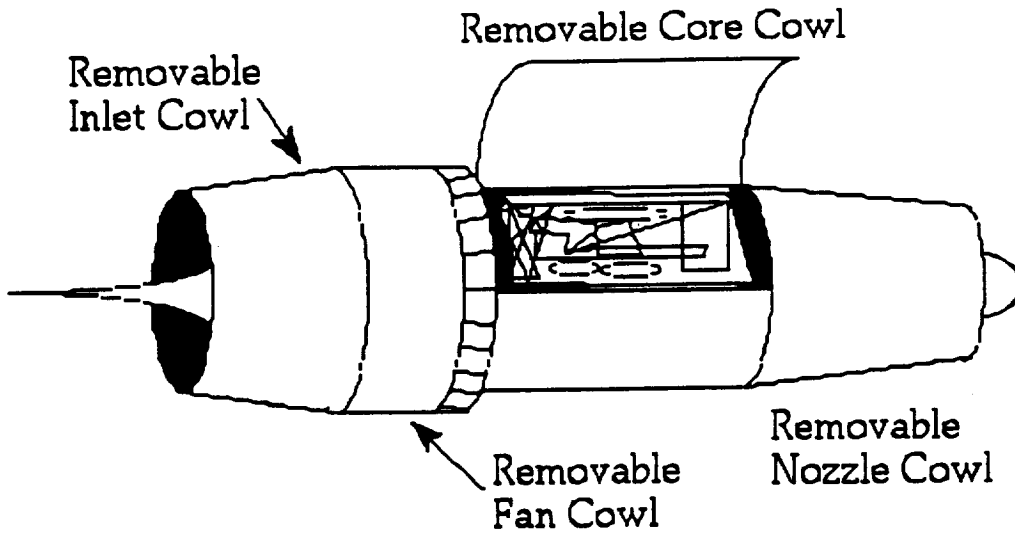


**Figure 14.2.2: Engine Access Panels**

Accessing vital components in the fuselage is as easy as reaching those on the wing. The auxiliary power unit, air-conditioning packs, and avionics bay are some systems that are easy to access from outside the fuselage. Access to these systems is shown in Figure 14.2.3. This view is the underside of the fuselage.

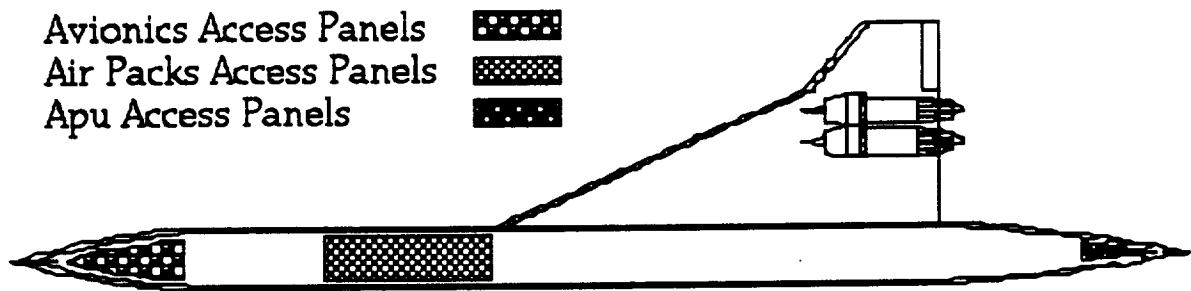
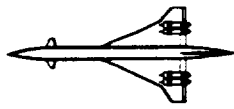


**Figure 14.2.3: Major Fuselage Access Panels**



## 15.0 Cost Analysis

### 15.1 Life Cycle Cost

Cost analysis was performed using two separate methods as provided in Reference 5 and 15. Due to the uniqueness of supersonic transports, the accuracy of the equations is unknown. Though limited data is available to determine actual economic feasibility of a second generation high speed civil transport, the values from the two methods were analyzed to generate conservative price estimations. The total cost required over the life of the aircraft was determined. The life cycle cost is defined as :

- Research, Development, Test, and Evaluation (RDT&E)
- Manufacturing and Acquisition
- Special Construction
- Operation and Support
- Disposal

The life cycle cost method was determined from statistical methods from Reference 15 in which 1989 dollars were converted to 2000 dollars also using a cost escalation factor. Values calculated from Reference 5 were used to verify estimated components of the life cycle cost. The life cycle cost determined for a 15 year period is shown in table 15.1.1.

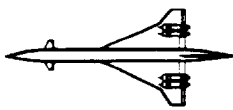


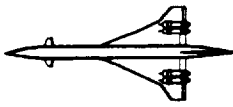
**Table 15.1.1: LCC Breakdown per Aircraft (in millions of 2000 dollars)**

Research, Development, Test, and Evaluation	11.82
Manufacturing and Acquisition	102.27
Operation and Support	824.82
Disposal	-12.55
Total	926.36

**Aircraft Price (with 10% manufacturer profit)      \$125.51 million**

Research, development, test and evaluation consists of 1.28% of the life cycle cost. It is assumed that 5 test aircraft are needed due to the unique design of Phoenix. Manufacturing and acquisition consists of 11.0% of the life cycle cost. A fleet size of 500 aircraft was used to calculate manufacturing costs. Special construction cost is neglected due to the fact that Phoenix was designed to operate within current airport infrastructures without any special modifications. Operation and support consisted of 89.0% of the life cycle cost. This is due the high direct operating cost (DOC) and indirect operating cost (IOC). The DOC break down is shown in Figure 15.2.1 and it was estimated that IOC was half of the DOC. The final life cycle cost was disposal which reduced the overall life cycle cost by 1.35%. This was due to the fact that the aircraft's value at the end of 15 years was assumed to have a salvage value of 10% of the original purchase price. The resulting graphical representation of





life cycle cost is shown in Figure 15.1.1 and 15.1.1. The resulting aircraft purchase price of \$125.5 million was determined from the RDT&E and manufacturing and acquisition costs with a 10% profit for the manufacturer.

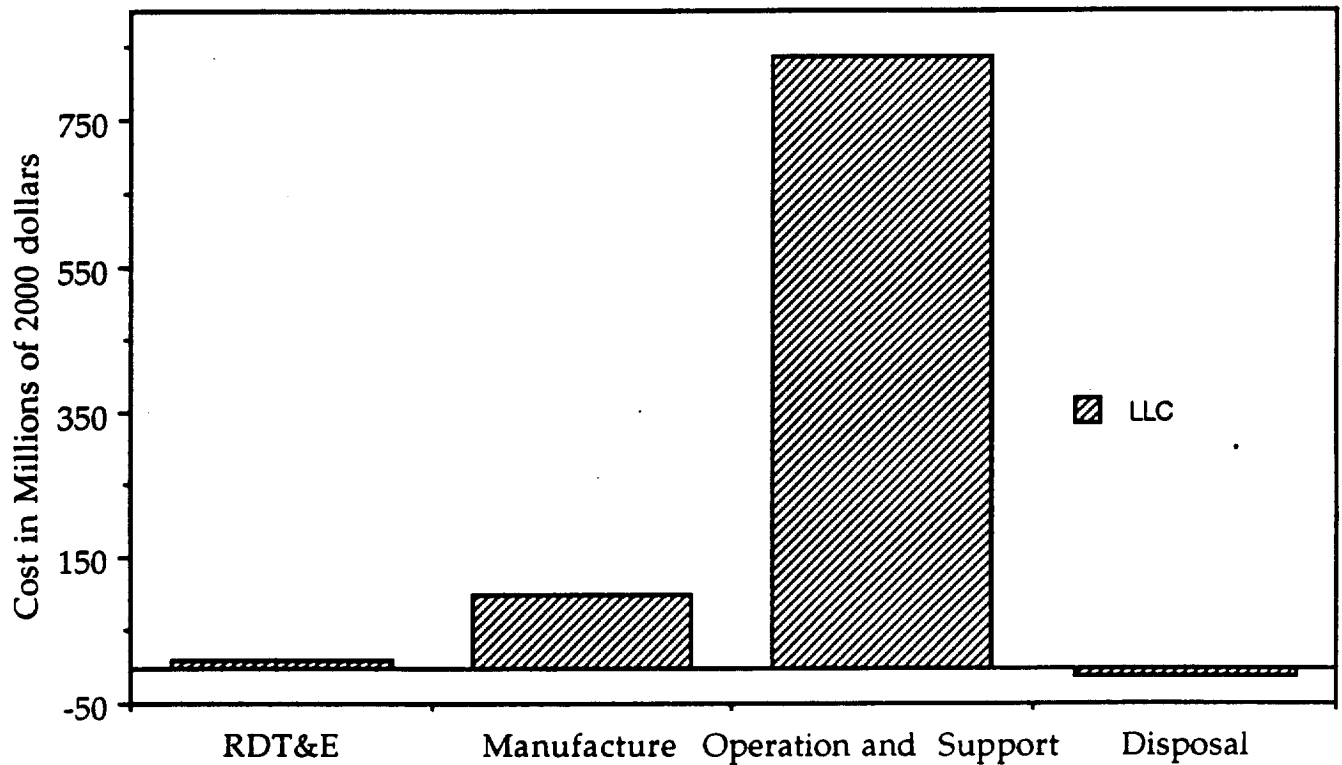


**Figure 15.1.1: Life Cycle Cost Breakdown**

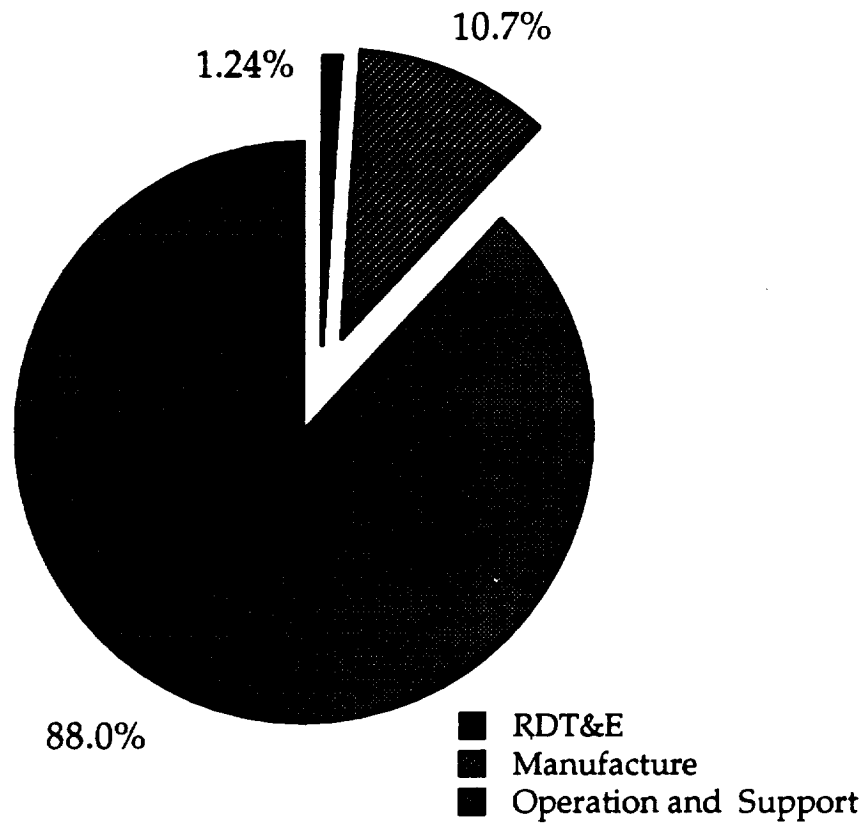
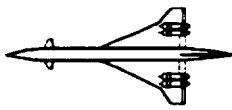


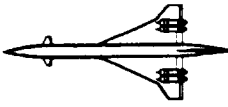
**Figure 15.1.2: Life Cycle Cost Percentage Breakdown**

### 15.2 Operation and Support

Direct operating costs consist of the following:

- Crew Cost
- Fuel Cost
- Maintenance and Material Costs
- Depreciation
- Insurance

Crew costs were calculated from 1989 dollars and scaled to year 2000 dollars. Fuel cost were estimated using a fuel price of 90 cents per



gallon. Crew and fuel costs consist of 59.2%. It is noticed that the fuel cost for the Phoenix is higher compared to the subsonic civil transports. This is due to the fact that supersonic transports fuel weight is approximately half of the takeoff weight while for a subsonic aircraft, it is approximately a third of the total takeoff weight. Maintenance and material cost consist of 25.7%. A correction factor of 1.8 was used to account for the manufacturing of non-conventional materials. An additional correction factor of 2.0 was used to account for an aggressive use of advanced technology.

Depreciation consist of 13.94% of the aircraft DOC and was determined from a straight line method over 15 years with a 10% aircraft salvage value. Insurance consist of only 1.34% and was estimated as a fraction of the total DOC. The resulting DOC per seat nautical mile of a block range of 5150 nautical miles is 8.4 cents. The actual DOC are shown in Table 15.2.1. The breakdown of the direct operating costs is shown in Figure 15.2.1

**Table 15.2.1: DOC per aircraft-year (millions in 2000 dollars)**

Crew and Fuel Cost	30.0
Maintenance and Material Costs	13.0
Depreciation	7.08
Insurance	0.682

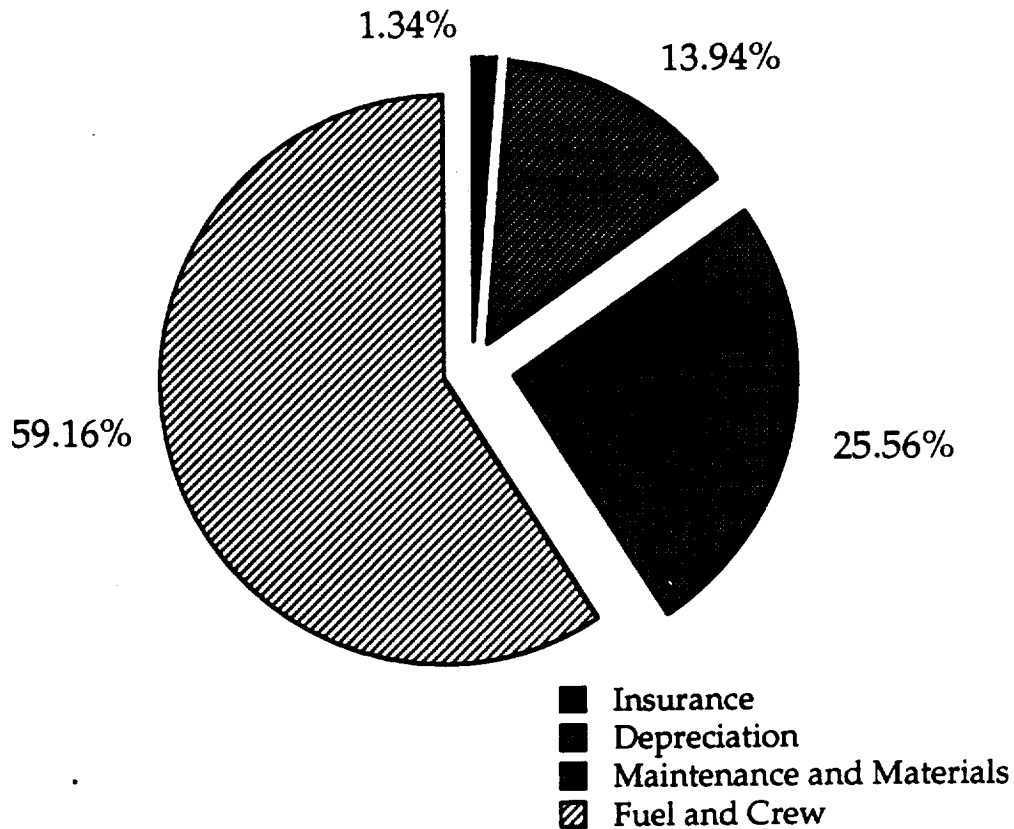
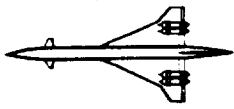
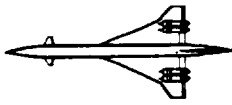


**Figure 15.2.1: Direct Operating Cost Breakdown**

Indirect operating costs consist of the following:

- Depreciation Cost of Grounds facilities and equipment
- Sales and Customer Service Costs
- Administrative and Overhead Costs

The value used is estimated to be half of the DOC. Using the DOC and IOC, the amount needed to pay off the aircraft in five years, a load factor of 65%, and a 10% profit, the resulting required one way ticket fare for a city pair of Los Angeles to Tokyo would be \$1530 per passenger.

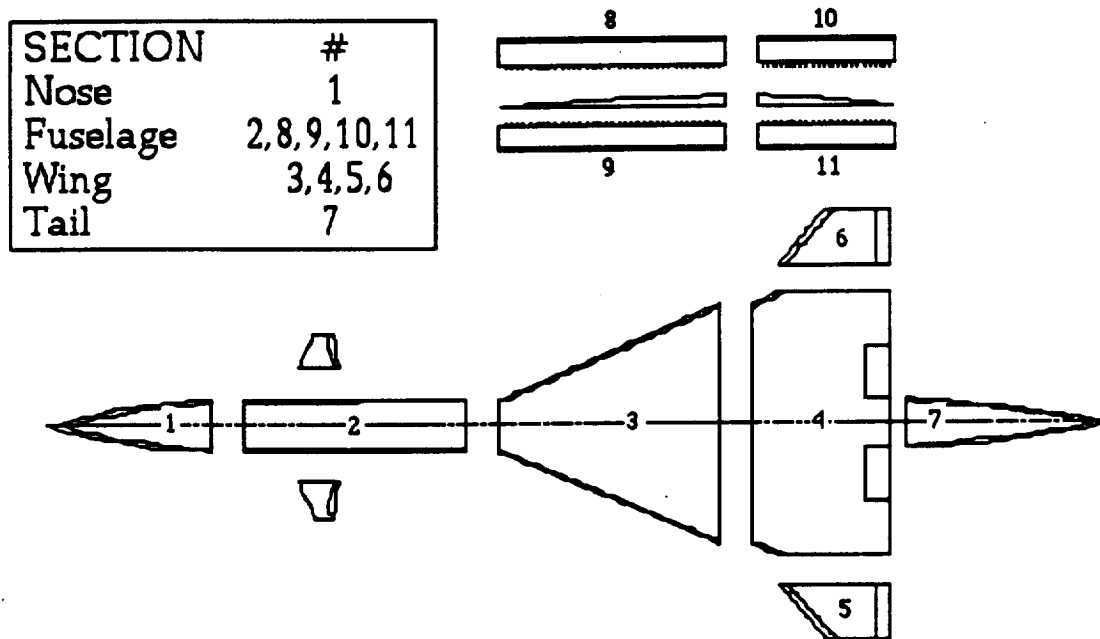


## 16.0 Manufacturing and Production Breakdown

### 16.1 Manufacturing

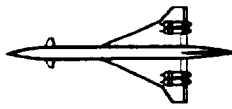
The manufacturing cost for one aircraft is 125.5 million dollars, as is shown in cost analysis. In order to keep the costs low, simple manufacturing methods are utilized. The airframer will subcontract out much of the work, as is done for subsonic aircraft. Subcontracted parts will arrive at the assembly line only when they are ready to be integrated into the airframe. Sub-assemblies will be used in order to help facilitate subcontracting and manufacturing of the aircraft.

Figure 16.1.1 shows the primary subassemblies of the HSCT.



**Figure 16.1.1: Manufacturing Breakdown**

The first phase of production will be the assembling of the



fuselage subassemblies and the wing subassemblies. The next phase will consist of the joining of the fuselage and wing. The installment of the control surfaces, engines, and major systems will complete the bulk of the aircraft assembly.

## 16.2 Production Schedule

Research and development will take many years in the design of the HSCT. It will take additional years to build and certify the first prototypes. After certification, the production schedule can begin in earnest. Producing 500 aircraft can be achieved in less than five years following the schedule in Table 16.2.1 below.

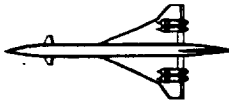
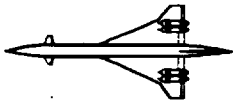


**Table 16.2.1: Production Schedule**

Month	Year	Production Rate
1	1	1
2	1	2
3	1	4
4	1	4
5	1	6
6-12	1	8
13-24	2	10
25-36	3	10
37-48	4	10
49-54	5	10
55	5	7

The first year sees the fewest aircraft produced because of the start up time and corrections that may need to be made if problems arise in the production aircraft.



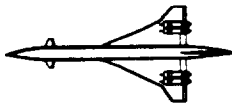
## **17.0 Conclusions**

The Phoenix aircraft is designed to fulfill an opening market for supersonic service to the Pacific Rim area in the 21st century. A design philosophy of simplicity and adaptability has yielded an aircraft of future economic and operational viability.

While this report demonstrates the means by which Phoenix can address the growing market, some in depth questions still remain to be answered by this design. Such subjects as stability and control indicate a problem in dynamic lateral stability to exist, yet gives general reliance upon an SAS to provide for these problems. A more thorough investigation into the effects of loop closure by such methods as Neal-Smith analysis or application of the Bandwidth criterion is needed to obtain better insight into the existent problems and to determine an exact solution to each. Other problems in this design are left to industry in general to provide solutions. This case is especially prominent in the propulsion and materials aspect of the Phoenix design. The engine industry is left in charge of fulfilling present and future noise, TSFC, and emission requirements for which this aircraft must operate.

Assumptions in material technology have shown benefits in weight sizing of this design, yet the actual benefits are not to be realized until industry is able to meet these expectations. Questions regarding wing-canard interactions at high Mach numbers need to be more deeply investigated to validate the assumed lift and performance capabilities of

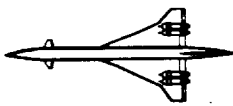




# *Phoenix*

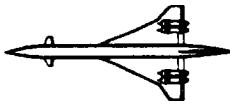
this aircraft. These are only some of the more prominent questions still needing to be addressed before Phoenix can make the step from conceptual design to actuality.

As with any design, improvements will always be sought and further research needing to be done. Even in regard to the limited scope of this report, the Phoenix still demonstrates itself to be a high contender in the growing market discussed by this report. Realistically, some reliance upon a strengthening technological base will always be required for advancements in engineering to be made. With great confidence, the Phoenix is sure to ride the forefront of these advances into the 21st century and beyond.



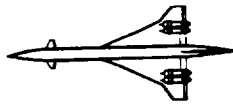
## 18.0 References

- 1 Carlson, H., The Lower Bound of Obtainable Sonic Boom Overpressure and Design Methods of Approaching this Limit, NASA TN D-1494, 1962
- 2 Roskam, Jan, Airplane Design: Part I. Preliminary Sizing of Airplanes, Roskam Aviation and Engineering Corporation, (Kansas, 1988)
- 3 Design Class, Compilation of the Research of the Airline Group, California Polytechnic State University
- 4 Mizuno, H., and Hagiwara, S., Feasibility Study on the Second Generation SST, 1991
- 5 Raymer, Daniel P., Aircraft Design: A Conceptual Approach, American Institute of Aeronautics and Astronautics, Inc., (Washington, D.C., 1989)
- 6 Coe, Paul L., Smith, Paul M., and Parlett, Lysle P., Low-Speed Wind Tunnel Investigation of an Advanced Supersonic Cruise Arrow-Wing Configuration, Langley Research Center, (Virginia, 1977)
- 7 Ashley, H. and Landahl, M., Aerodynamics of Wings and Bodies, Dover Publications, Inc., (New York, 1985)
- 8 High-Speed Civil Transport Study, Boeing Commercial Airplanes, NASA Contractor Report 4234, 1989
- 9 Kepler, C. E., and Champagne, G. A., Supersonic Through-Flow

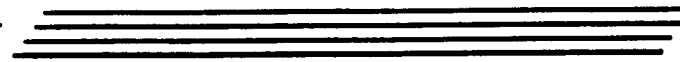
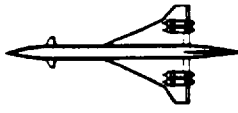


Fan Assessment, NASA Lewis Research Center

- 10 Gilkey, S. C., and Hines, R. W., Propulsion Perspective of the Second Generation Supersonic Transport, GE Engines and Pratt and Whitney, 1991
- 11 Roskam, Jan, Airplane Design: Part IV. Layout Design of Landing Gear and Systems, Roskam Aviation and Engineering Corporation, (Kansas, 1988)
- 12 Roskam, Jan, Airplane Design: Part V. Component Weight Estimation, Roskam Aviation and Engineering Corporation, (Kansas, 1988)
- 13 Roskam, Jan, Airplane Design: Part VI. Preliminary Calculation of Aerodynamic, Thrust, and Power Characteristics, Roskam Aviation and Engineering Corporation, (Kansas, 1988)
- 14 Roskam, Jan, Airplane Design: Part VII. Determination of Stability, Control and Performance Characteristics: FAR and Military Requirements, Roskam Aviation and Engineering Corporation, (Kansas, 1988)
- 15 Roskam, Jan, Airplane Design: Part VIII. Airplane Cost Estimation and Optimization: Design, Development, Manufacturing, and Operating, Roskam Aviation and Engineering Corporation, (Kansas, 1988)
- 16 Aluminum-Lithium Alloys Design, Development and Application Update, ASM International, 1988
- 17 FitzSimmons, R.D. and Roensch, R.L., Supersonic Transport, SAE. Inc.



- 18 FitzSimmons, R.D., and Rowe, W.T., AST Propulsion Comparisons, SAE, Inc.
- 19 Franciscus, L. C., and Maldonado, J. J., Supersonic Through-Flow Fan Engine and Aircraft Mission Performance, AIAA-89-2139, July 1989
- 20 Manro, Marjorie E., Bobbitt, Percy J., and Kulfan, Robert M., The Prediction of Pressure Distributions on an Arrow-Wing Configuration Including the Effect of Camber, Twist, and A Wing Fin, NASA Langley Research Center
- 21 Roensch, R.L., Felix, J.E., and Welge, H.R., Results of a Low-Speed Wind Tunnel Test of the MDC 2.2M Supersonic Cruise Aircraft Configuration, Douglas Aircraft Company
- 22 Roensch, R. L., and Page, G.S., Analytical Development of an Improved Supersonic Cruise Aircraft Based On Wind Tunnel Data, Douglas Aircraft Company
- 23 Roskam, Jan, Airplane Design: Part II. Preliminary Configuration Design and Integration of the Propulsion System, Roskam Aviation and Engineering Corporation, (Kansas, 1988)
- 24 Roskam, Jan, Airplane Design: Part III. Layout Design of Cockpit, Fuselage, Wing, and Empennage: Cutaways and Inboard Profiles, Roskam Aviation and Engineering Corporation, (Kansas, 1988)
- 25 Roskam, Jan, Airplane Flight Dynamics and Automatic Flight Controls Part I, Roskam Aviation and Engineering Corporation, (Kansas, 1982)
- 26 Study of High Speed Civil Transports, Douglas Aircraft Company,



# *Phoenix*

NASA Contractor Report 4235, 1989